

Nuclear theory for exotic nuclei: selected topics

Youngman Kim
(Center for Exotic Nuclear Studies, IBS)

Tongji U., May 8, 2024

Domestic collaborators at IBS

- CENS: Myungkuk Kim, Igor Mazur, Soonchul Choi,
Myunghee Park, (Qiang Zhao, moved to Osaka)
- IRIS: Young-Ho Song, Ik Jae Shin, Kyungil Kim,
Panagiota Papakonstantinou

Contents

- Ab initio NCSM and Daejeon 16 N-N interaction
- Nuclear Lattice Effective Field Theory
- Covariant density functional theory
- Summary

Ab initio NCSM

- Ab initio: nuclei from first principles using “fundamental” interactions without uncontrolled approximations.
- No core: all nucleons are active, no inert core.
- Shell model: harmonic oscillator basis
- Point nucleons

- A -nucleon Schrödinger equation

$$\hat{H} \Psi(r_1, \dots, r_A) = E \Psi(r_1, \dots, r_A)$$

- Hamiltonian with $NN(+NNN)$ interactions

$$\hat{H} = \frac{1}{A} \sum_{i < j} \frac{(\vec{p}_i - \vec{p}_j)^2}{2m} + \sum_{i < j} V_{ij} + \sum_{i < j < k} V_{ijk} + \dots$$

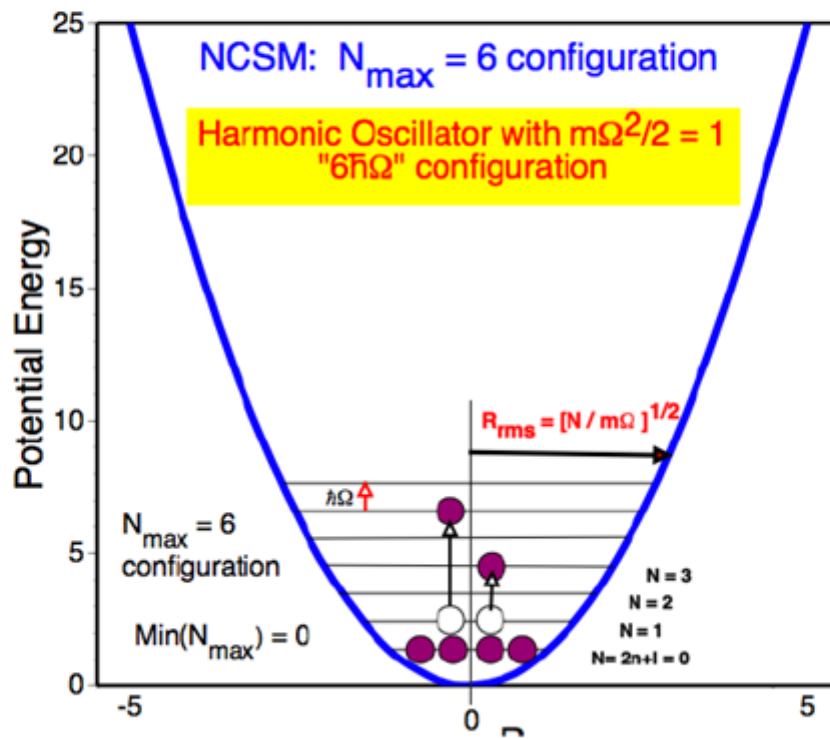
- Wave functions are expanded in basis states

$$\Psi(r_1, \dots, r_A) = \sum a_i \Phi_i(r_1, \dots, r_A)$$

basis states Φ_i : Slater determinants of single particle states

- single particle states ϕ
for radial wave functions, harmonic oscillators are used

$$\Rightarrow \Phi_i \sim \phi_1^{(i)} \times \phi_2^{(i)} \times \cdots \times \phi_A^{(i)}$$



from the talk by J. Vary @ RISP, Mar. 2013

${}^6\text{Li}$	Exp.	NNLO _{opt}	JISP16	JISP16*	AV18/IL2
$E_{\text{gs}}(1^+, 0)$	31.995	30.55(9)	31.53(2)	31.49(3)	32.0(1)
$\langle r_{pp}^2 \rangle^{1/2}$	2.38(3)	2.40(3)	2.28(3)	2.3	2.39(1)
$E_x(3^+, 0)$	2.186(2)	2.843(1)	2.560(3)	2.56(2)	2.2(2)
$E_x(0^+, 1)$	3.56(1)	3.879(15)	3.708(6)	3.68(6)	3.4(2)
$E_x(2^+, 0)$	4.312(22)	4.36(9)	4.63(10)	4.5(3)	4.2(2)
$E_x(2^+, 1)$	5.366(15)	6.19(6)	6.07(6)	5.9(2)	5.5(2)
$Q(1^+, 0)$	-0.082(2)	-0.032(7)	-0.078(3)	-0.077(5)	-0.32(6)
$Q(3^+, 0)$	-	-5.1(3)	-4.8(2)	-4.9	
$\mu(1^+, 0)$	0.822	0.8380(5) [†]	0.8389(2)	0.839(2)	0.800(1)
$\mu(3^+, 0)$	-	1.8607(1) [†]	1.8654(1)	1.866(2)	
$B(\text{E2};(3^+, 0))$	10.7(8)	6.4(6)	5.8(4)	6.1	11.65(13)
$B(\text{E2};(2^+, 0))$	4.4(23)	6.6(7) [†]	6.7(7)	7.5	8.66(47)
$B(\text{M1};(0^+, 1))$	15.43(32)	14.59(8)	14.25(4)	14.2(1)	15.02(11)
$B(\text{M1};(2^+, 1))$	0.15	0.031(3)	0.042(3)	0.05(1)	
M_{GT}	2.170	2.260(4)	2.225(2)	2.227(2)	2.18(3)

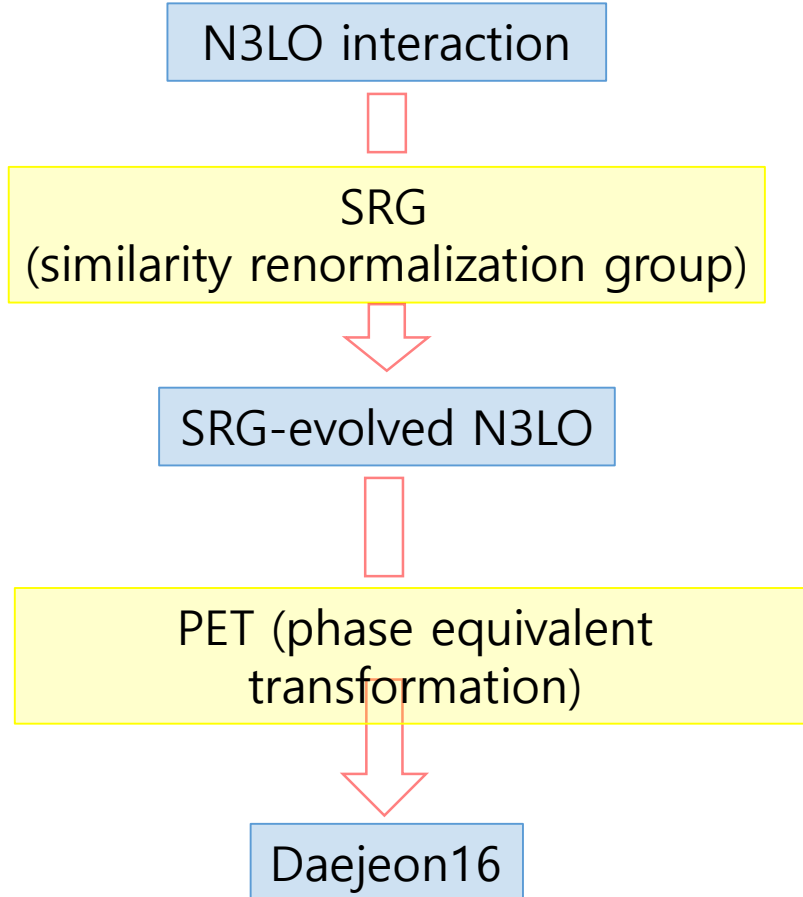
Ab initio structure and NN interaction

- Unfortunately, the NN interaction at low energies needed for nuclear physics applications cannot be directly derived from QCD at the moment
- Ab initio theory requires, of course, a realistic NN interaction accurately describing NN scattering data and deuteron properties
- Nice to avoid NNN forces? Yes

≈30 times more
Hamiltonian matrix
elements when *NNN*
forces are involved;
hence much more
computer resources
are required for
calculations

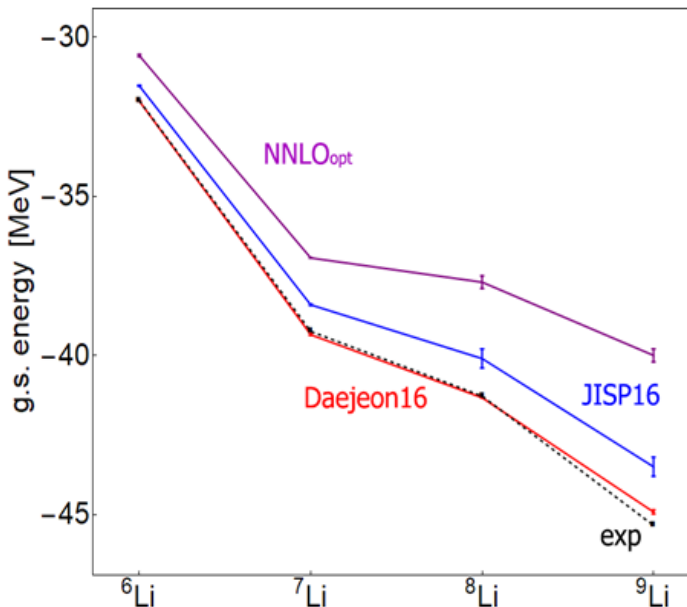
Daejeon 16 NN interaction

Used in many ab initio structure studies and more are planned



Ground state energies of Li isotopes

calculated w/ JISP16, NNLO_{opt} and Daejeon16
compared to experimental data.



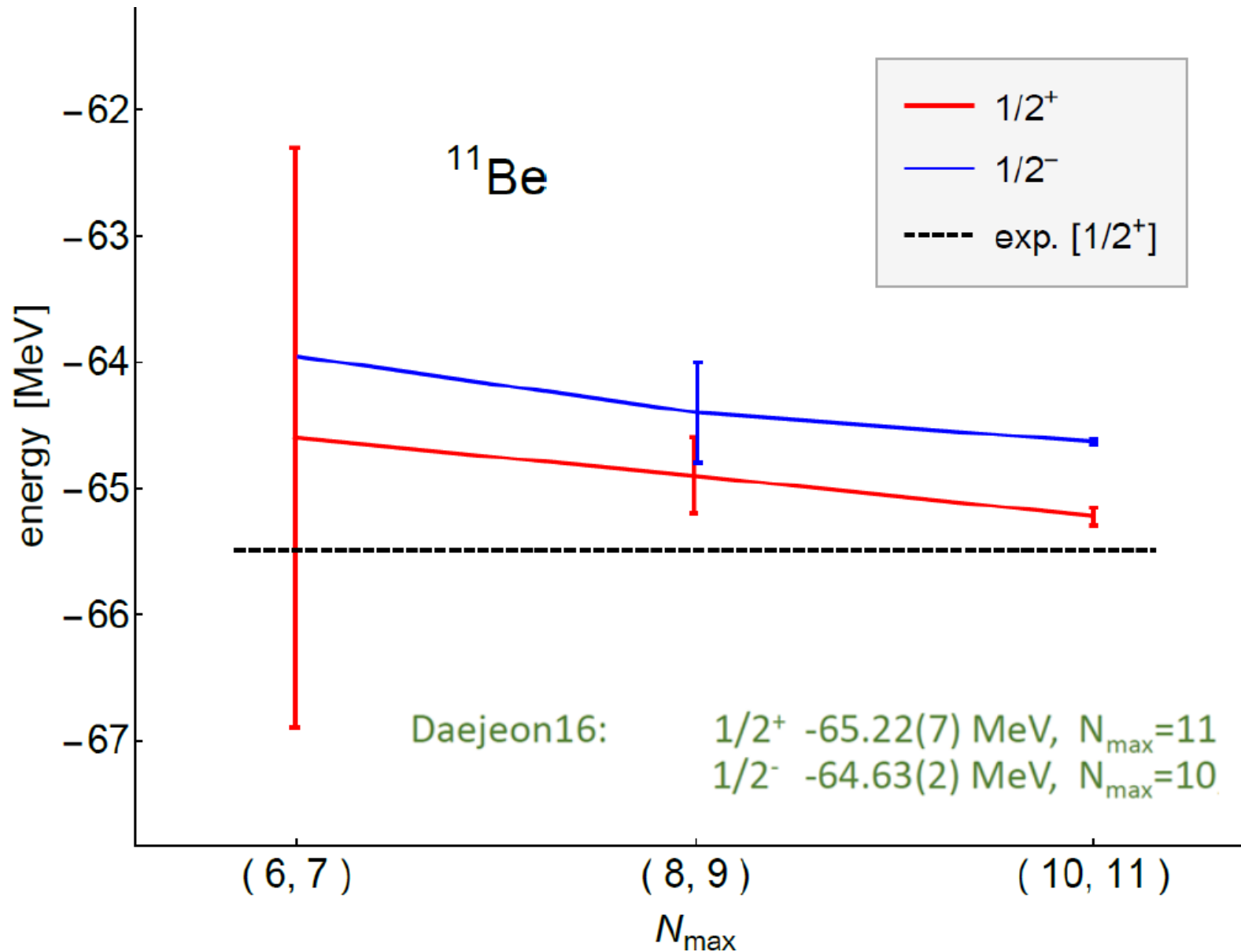
- Daejeon16 shows more excellent description for the binding energies of Lithium isotopes than NNLO_{opt} (from the first principle) and JISP16 (phenomenological.)
- For each result, extrapolation is adopted.
- ${}^6\text{Li} : \sim N_{\text{max}} = 18$
 ${}^7\text{Li} \sim {}^9\text{Li} : \sim N_{\text{max}} = 10$

Nucleus	Nature	Daejeon16			JISP16		
		Theory	$\hbar\Omega$	N_{\max}	Theory	$\hbar\Omega$	N_{\max}
^3H	8.482	$8.442(^{+0.003}_{-0.000})$	12.5	16	8.370(3)	15	20
^3He	7.718	$7.744(^{+0.005}_{-0.000})$	12.5	16	7.667(5)	17.5	20
^4He	28.296	28.372(0)	17.5	16	28.299(0)	22.5	18
^6He	29.269	29.39(3)	12.5	14	28.80(5)	17.5	16
^8He	31.409	31.28(1)	12.5	14	29.9(2)	20	14
^6Li	31.995	31.98(2)	12.5	14	31.48(3)	20	16
^{10}B	64.751	64.79(3)	17.5	10	63.9(1)	22.5	10
^{12}C	92.162	92.9(1)	17.5	8	94.8(3)	27.5	10
^{16}O	127.619	131.4(7)	17.5	8	145(8)	35	8

Binding energies (in MeV) of nuclei obtained with Daejeon16 NN interaction using Extrapolation B with estimated uncertainty of the extrapolation.

Parity Inversion in ^{11}Be

- Experimentally: $1/2^+$ -65.483(6) MeV
 $1/2^-$ -65.165(7) MeV, Exc. energy 0.318(7) MeV
- JISP16: $1/2^+$ -63.3(8) MeV, $N_{\max}=11$
 $1/2^-$ -64.0(6) MeV, $N_{\max}=10$



Deep learning: Extrapolation tool for ab initio nuclear theory

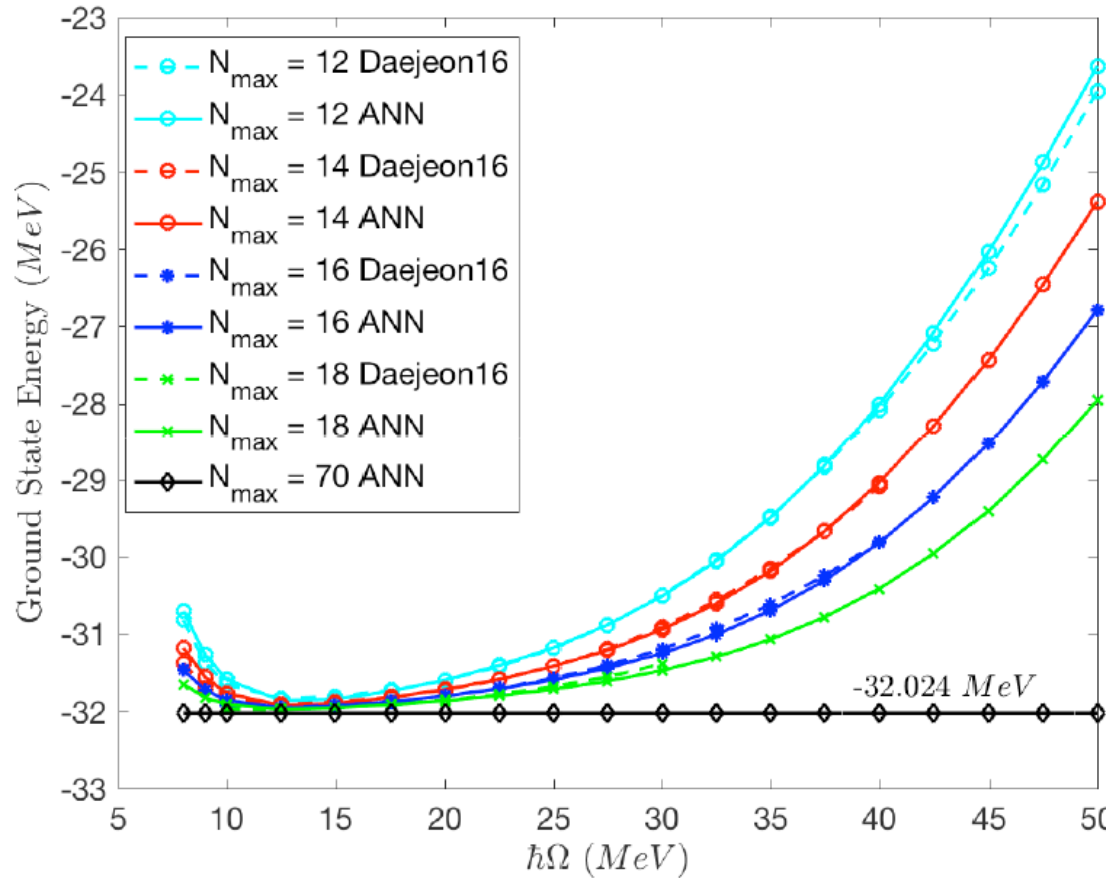


Figure 7. Comparison of the NCSM calculated and the corresponding ANN predicted gs energy values of ${}^6\text{Li}$ as a function of $\hbar\Omega$ at $N_{\max} = 12, 14, 16$, and 18 . The lowest horizontal line corresponds to the ANN nearly converged result at $N_{\max} = 70$.

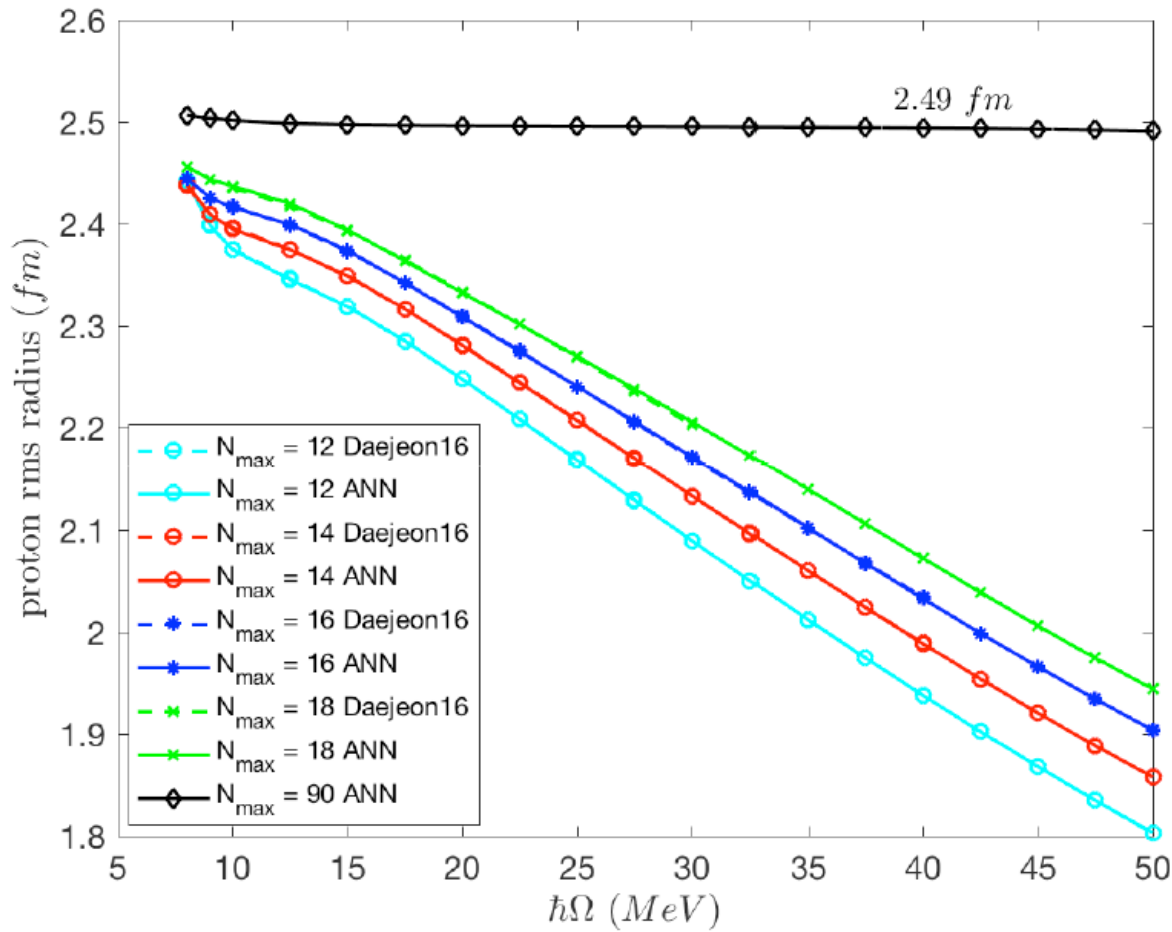
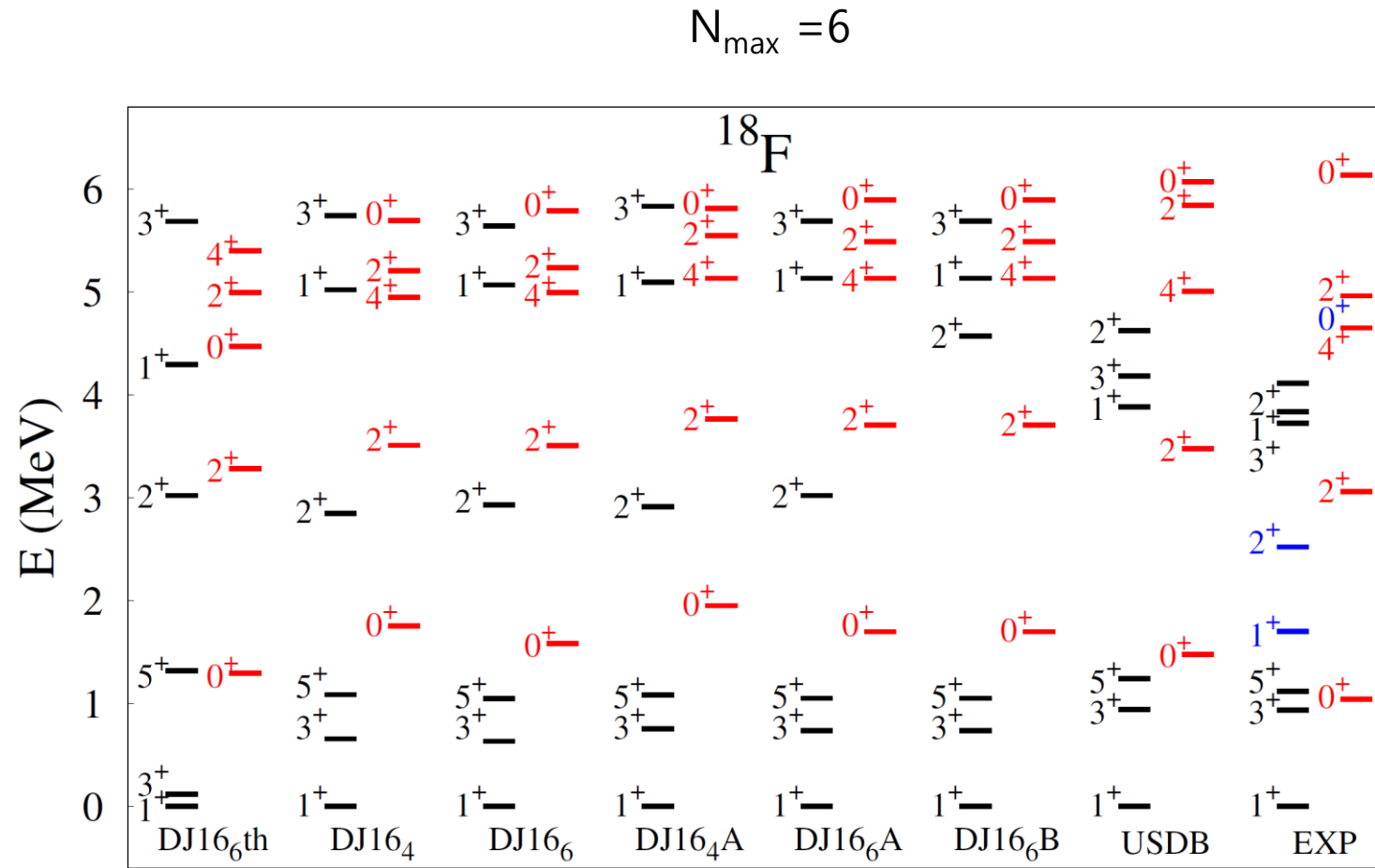


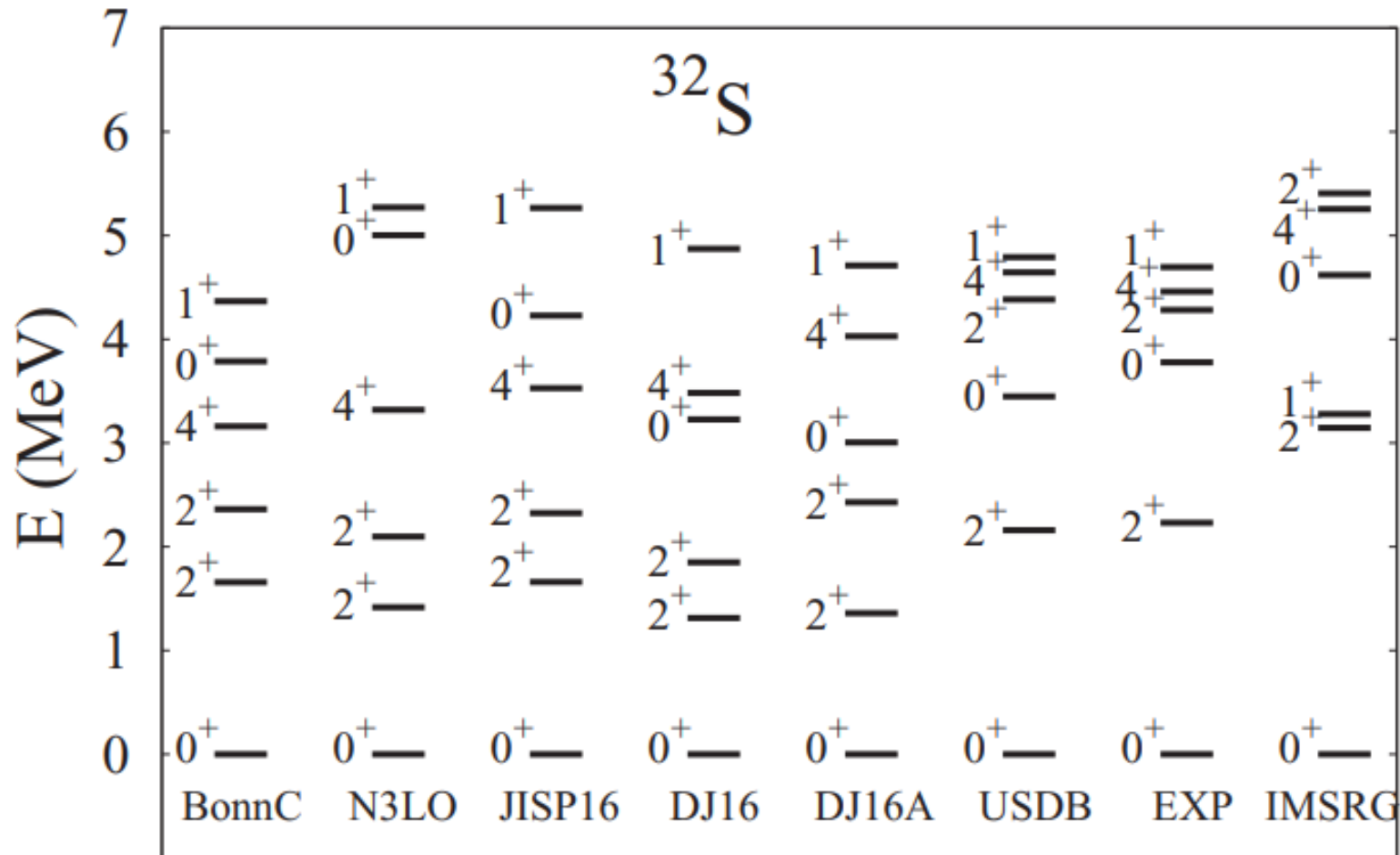
Figure 9. Comparison of the NCSM calculated and the corresponding ANN predicted gs point proton rms radius values of ${}^6\text{Li}$ as a function of $\hbar\Omega$ for $N_{\max} = 12, 14, 16$, and 18 . The highest curve corresponds to the ANN nearly converged result at $N_{\max} = 90$.

Effective shell-model interactions from Daejeon 16

A new (not fully though) microscopic effective shell-model interactions in the valence sd shell, obtained from the modern Daejeon16 nucleon-nucleon potential



$N_{\max} = 4$



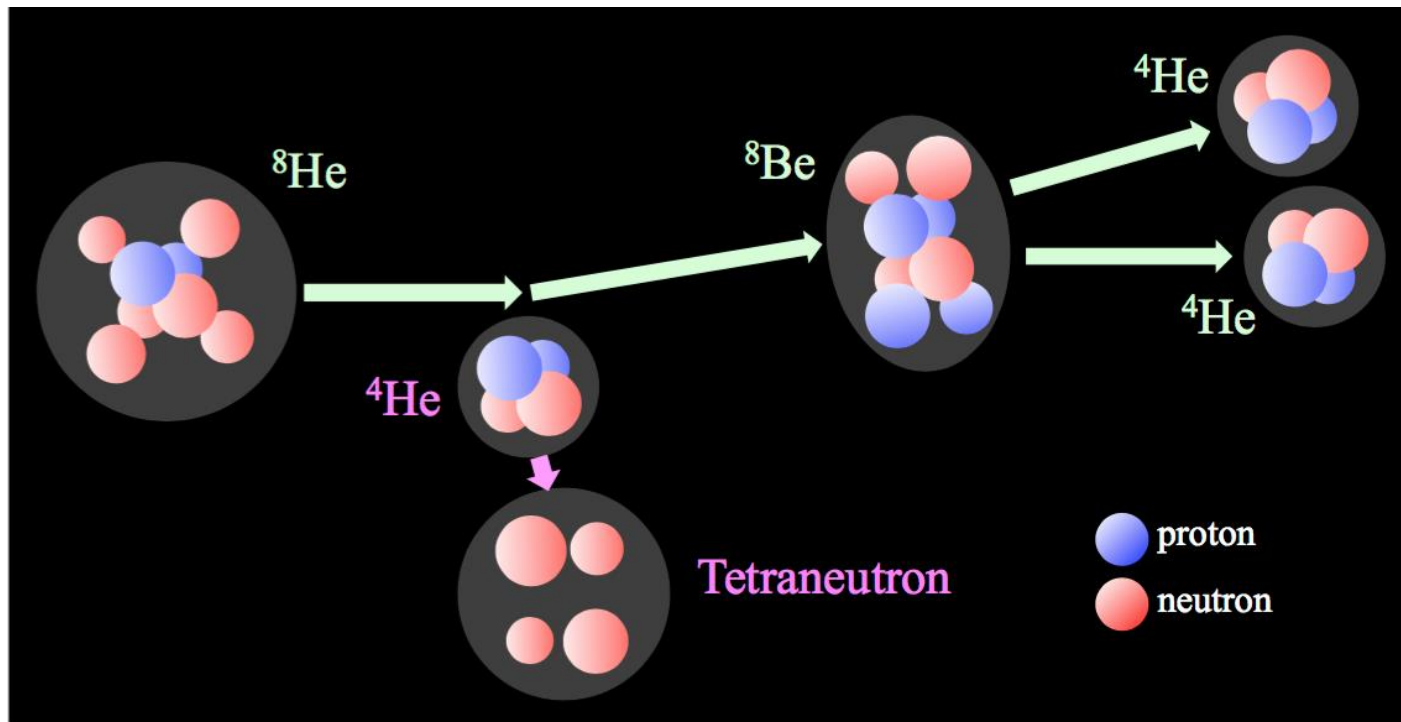
Application harmonic oscillator to continuum spectrum

Resonance		This work		Experiment
$J^\pi(^7\text{He})$	$J^\pi(^6\text{He})$	JISP16	Daejeon16	
$3/2^-_1$	0^+	E_r	0.665(12)	0.430(3)
		Γ	0.57(4)	0.182(5)
$1/2^+_1$	0^+	E_r		
		Γ		
$1/2^-_1$	0^+	E_r	2.7(8)	3.0(1)
		Γ	5.0(6)	2
$5/2^-_1$	0^+	E_r	4.4(4)	3.5
		Γ	1.56(4)	10
2^+_1		E_r	3.85(15)	1.0(1)
		Γ	2.5(2)	0.75(8)
Predictions		E_r	4.1(7)	3.36(9)
		Γ	2.0(7)	1.99(17)
$3/2^-_2$	0^+	E_r	5.8(5)	
		Γ	4.11(23)	
2^+_2		E_r	5.3(4)	
		Γ	3.9(6)	
Predictions		E_r	5.6(7)	
		Γ	4.0(7)	
			5.0(3)	
			2.84(24)	
			4.4(4)	
			3.9(3)	
			4.7(7)	
			3.4(8)	

We describe all experimentally known ${}^7\text{He}$ resonances and suggest an interpretation of an observed wide resonance of unknown spin-parity

I. A. Mazur, I. J. Shin, Y. Kim et al., SS-HORSE extension of the no-core shell model: Application to resonances in ${}^7\text{He}$, PRC 106, 064320 (2022)

Tetra neutron



K. Kisamori et al., Phys. Rev. Lett. **116**, 052501 (2016):
 $E_R = 0.83 \pm 0.63(\text{statistical}) \pm 1.25(\text{systematic}) \text{ MeV}$; width $\Gamma \leq 2.6 \text{ MeV}$

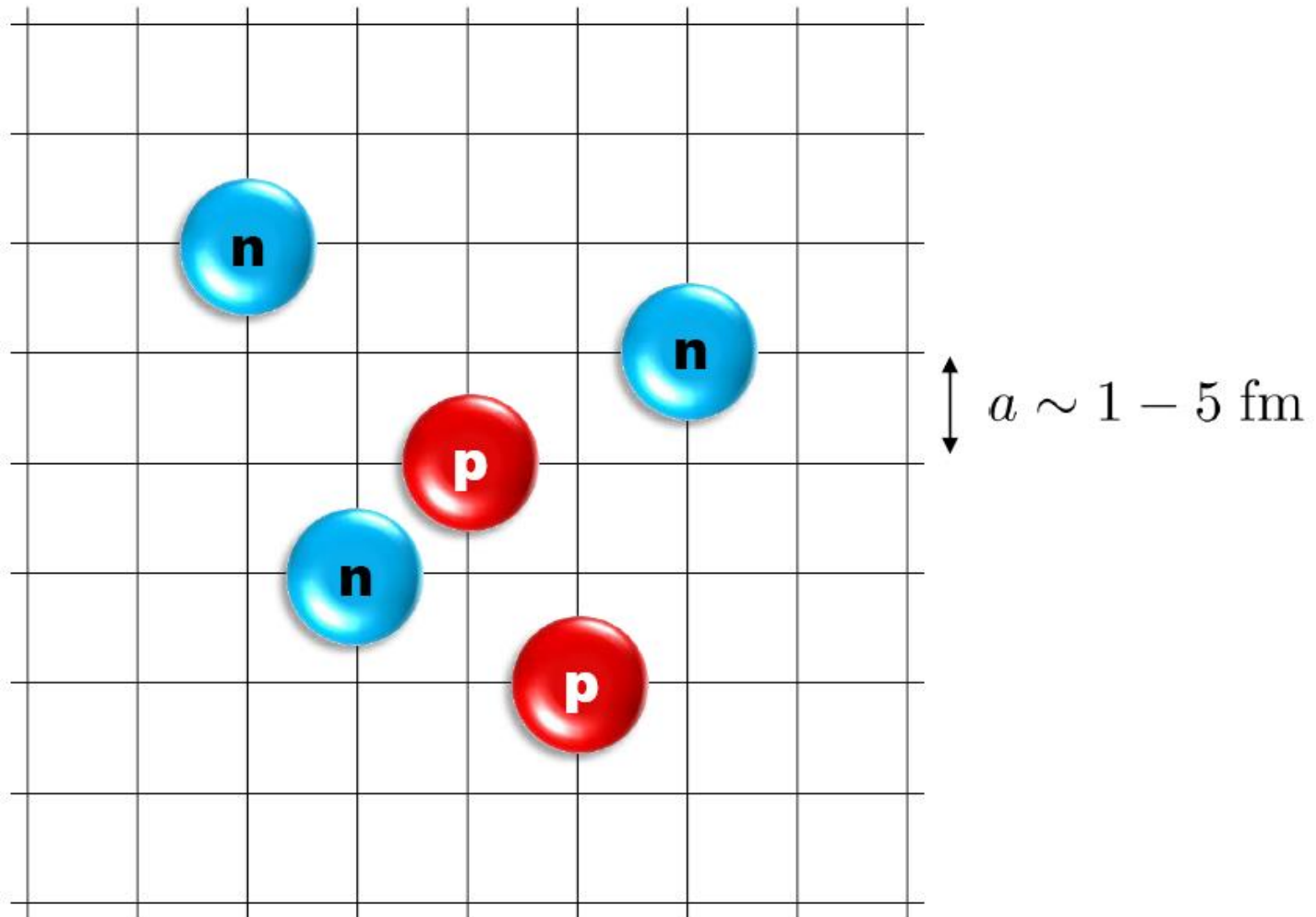
A.M. Shirokov, G. Papadimitriou, A.I. Mazur, I.A. Mazur, R. Roth, J.P. Vary. Phys. Rev. Lett. 117 (2016) 182502

JISP 16: $E_r=0.8 \text{ MeV}, \Gamma=1.4$

Interaction	JISP16	Daejeon16	Idaho N3LO, SRG	
			$\Lambda = 1.5 \text{ fm}^{-1}$	$\Lambda = 2.0 \text{ fm}^{-1}$
E_r [MeV]	0.844	0.997	0.783	0.846
Γ [MeV]	1.38	1.60	1.15	1.29

I. Mazur, A.M.Shirokov, I. A. Mazur, L. D. Blokhintsev, Y.Kim, I. J.Shin, and J. P. Vary, Physics of Atomic Nuclei 82, 537 (2019)

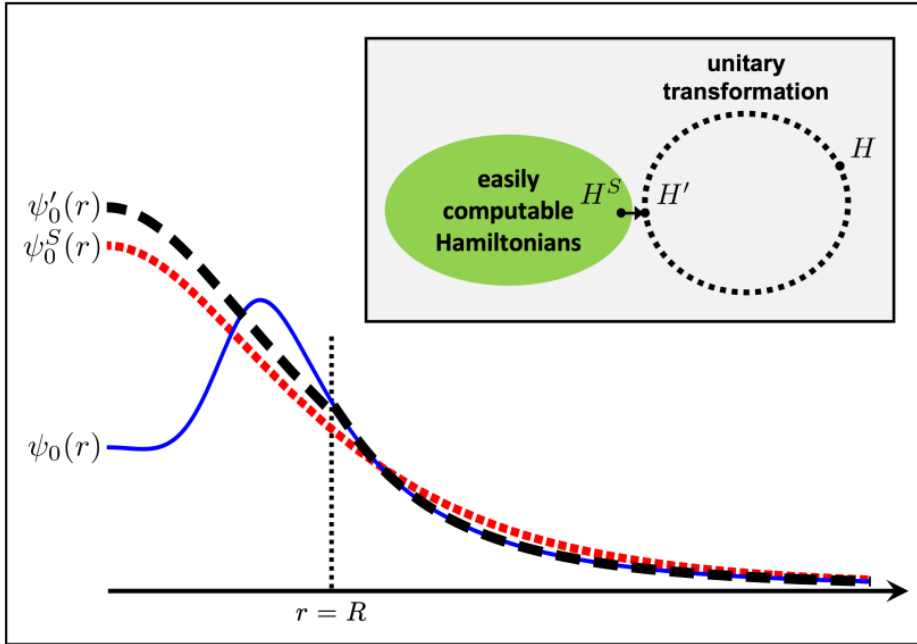
Lattice effective field theory



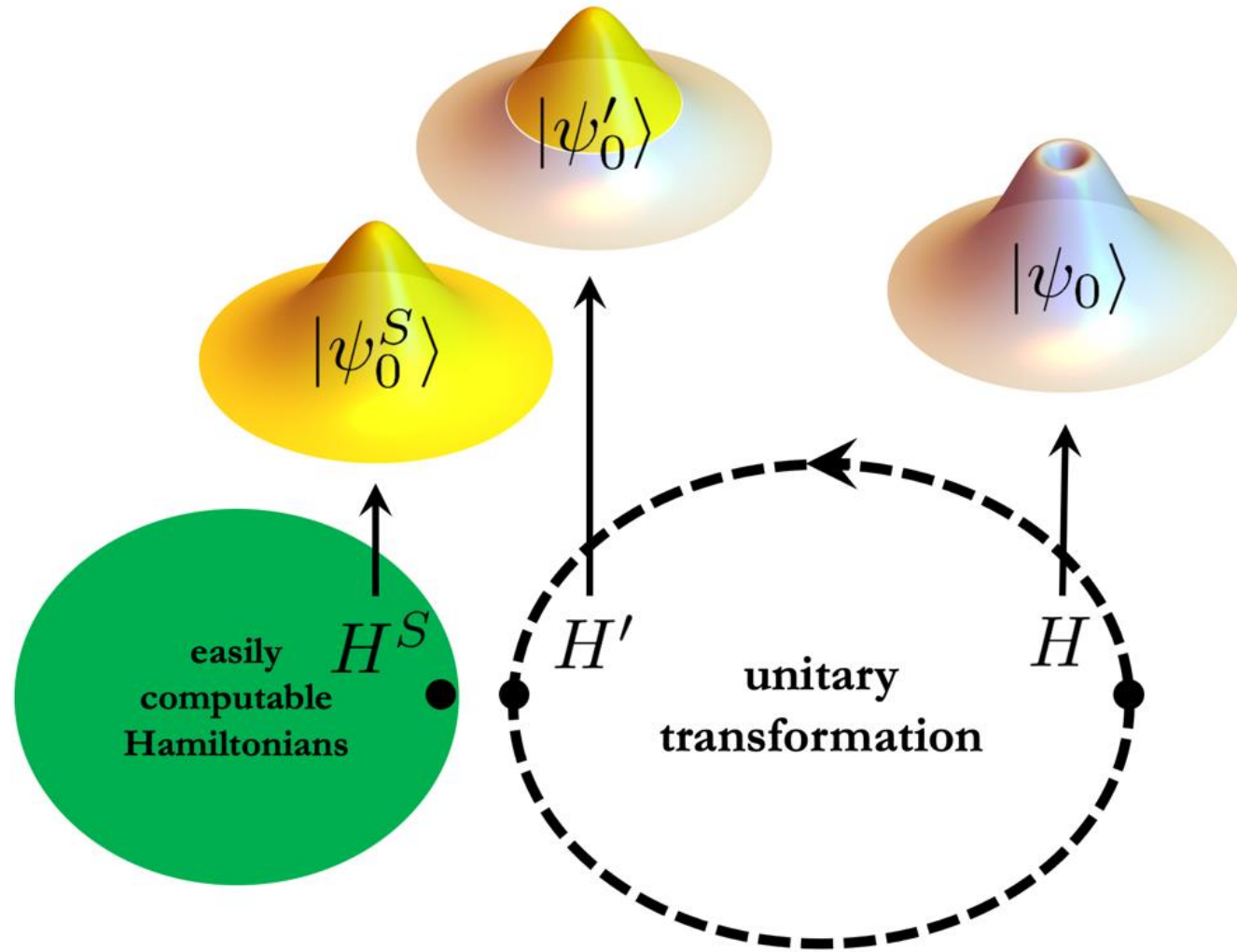
Wave function matching for the quantum many-body problem

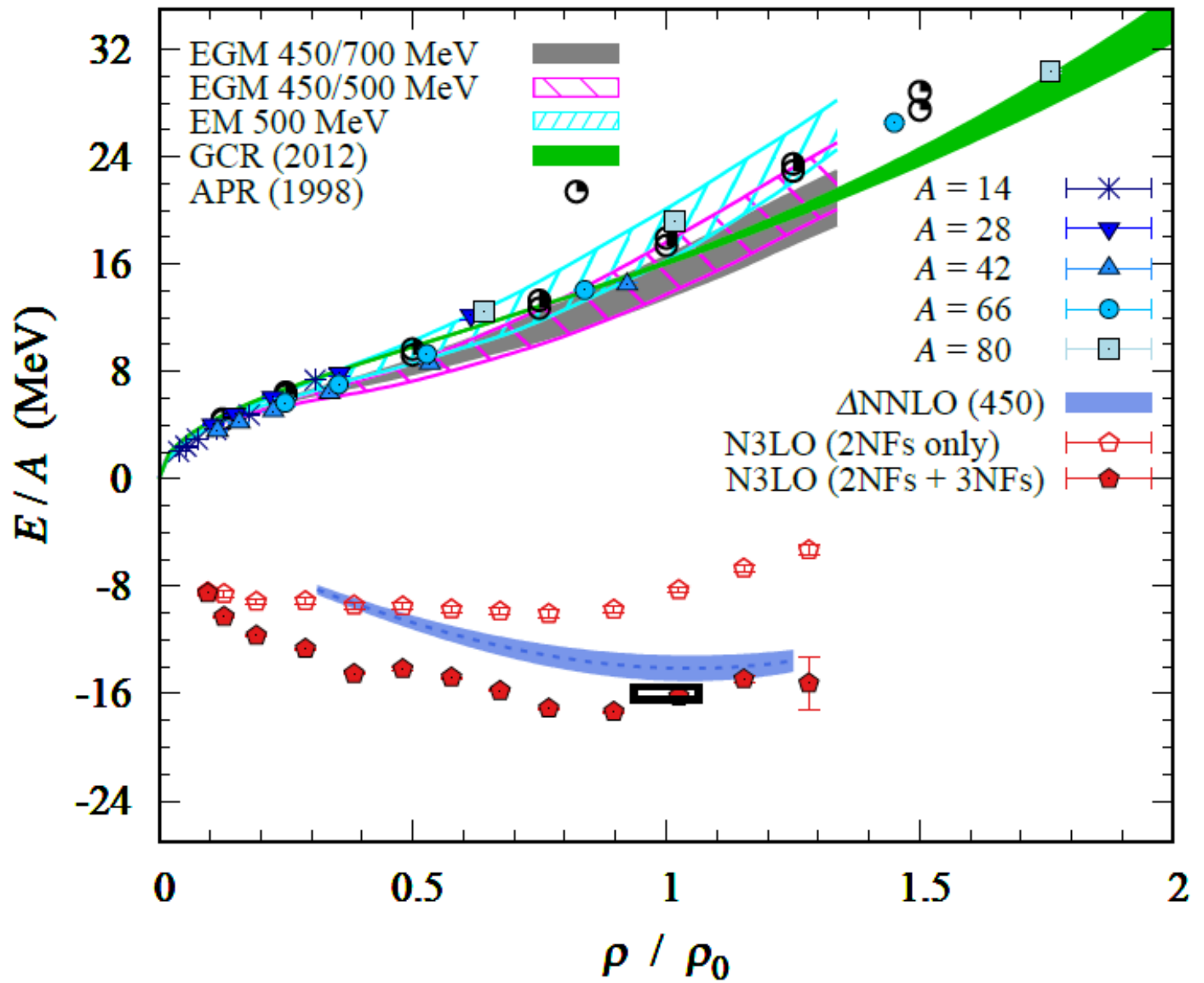
Serdar Elhatisari,¹ Lukas Bovermann,¹ Evgeny Epelbaum,¹ Dillon Frame,¹ Fabian Hildenbrand,¹ Myungkuk Kim,¹ Youngman Kim,¹ Hermann Krebs,¹ Timo A. Lähde,¹ Dean Lee,¹ Ning Li,¹ Bing-Nan Lu,¹ Yuanzhuo Ma,¹ Ulf-G. Meißner,¹ Gautam Rupak,¹ Shihang Shen,¹ Young-Ho Song,¹ and Gianluca Stellin¹

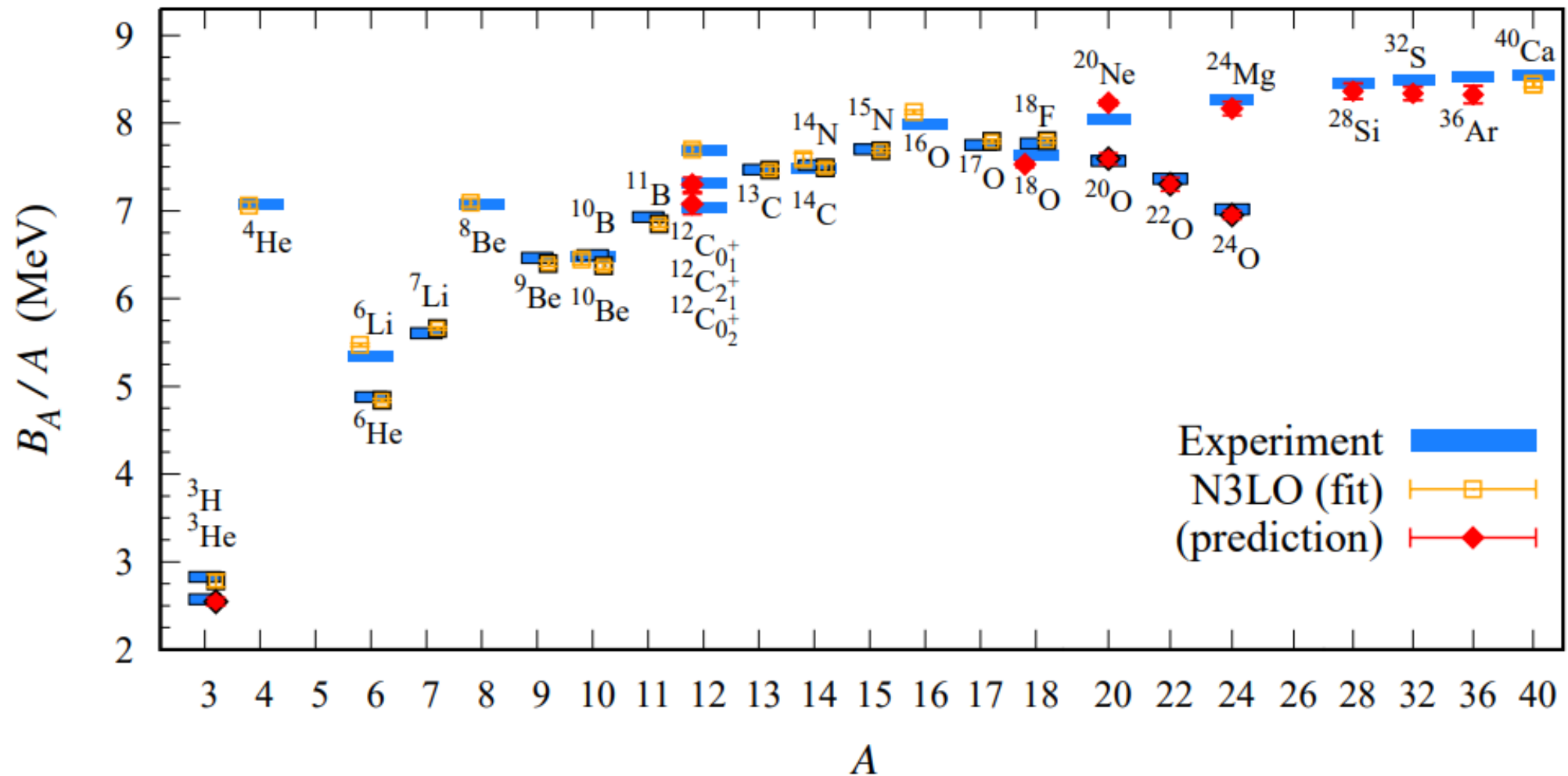
We introduce a new approach for solving quantum many-body systems called *wave function matching*. Wave function matching transforms the interaction between particles so that the wave functions at short distances match that of an easily computable interaction. This allows for calculations of systems that would otherwise be impossible due to problems such as Monte Carlo sign cancellations. We apply the method to lattice Monte Carlo simulations of light nuclei, medium-mass nuclei, neutron matter, and nuclear matter. We use interactions at next-to-next-to-next-to-leading order in the framework of chiral effective field theory and find good agreement with empirical data. These results are accompanied by new insights on the nuclear interactions that may help to resolve long-standing challenges in accurately reproducing nuclear binding energies, charge radii, and nuclear matter saturation in *ab initio* calculations.

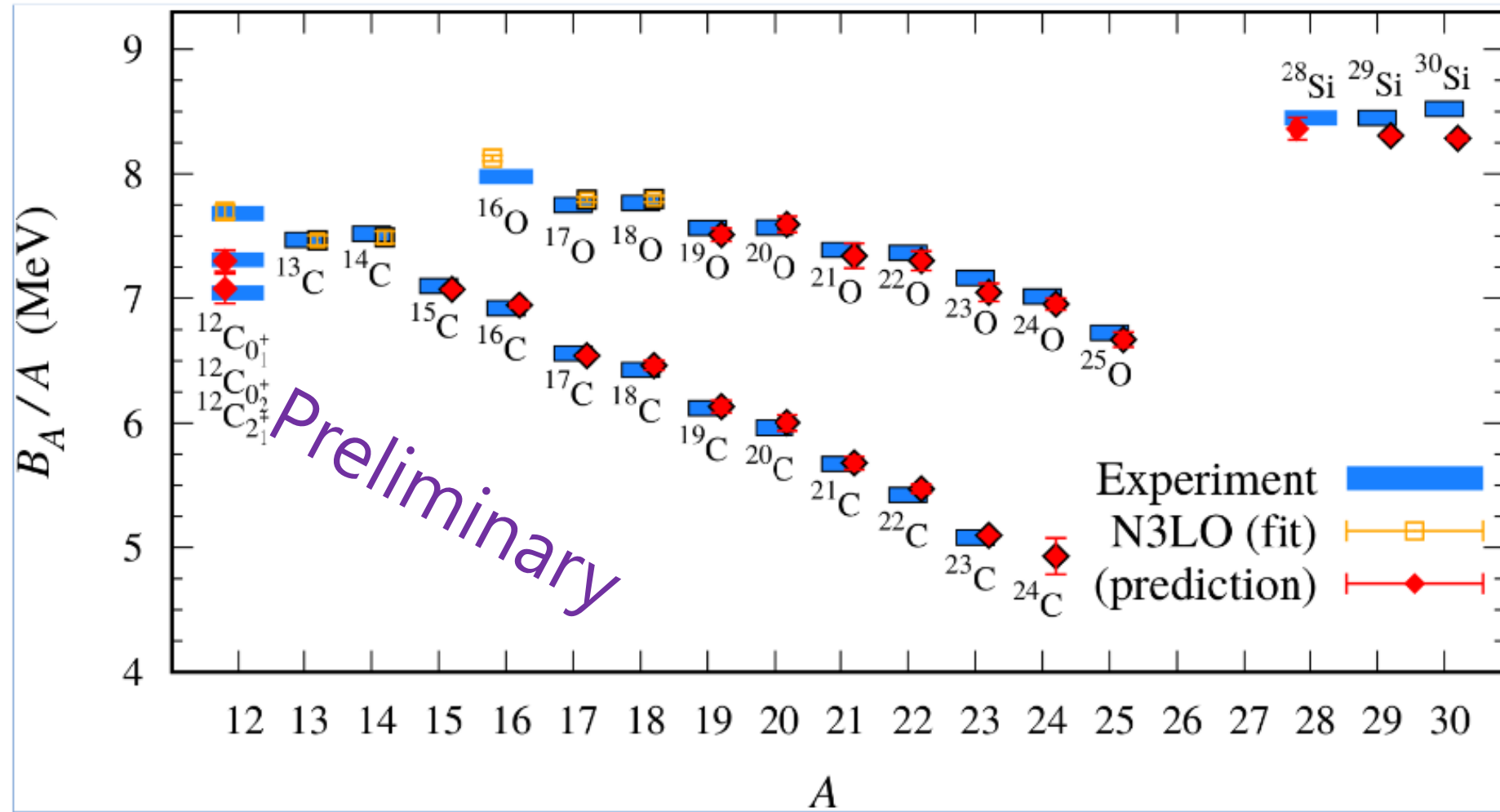


Suppose we have a simple and solvable Hamiltonian H^S and a realistic high-fidelity Hamiltonian H . Wave function matching enables us to construct a unitary transformation U through quantum adiabatic evolution that defines a new Hamiltonian H' from H such that the ground-state wave function of H' matches that of H^S at short distances, say $r < R$. For $r < R$ the unitary transformation is defined inactive and therefore the ground-state wave function of H' is the same with that of H . In this study we use the leading order chiral effective interaction for H^S and the next-next-next leading order ones for H . We take $R = 3.7$ fm.









Covariant density functional theory



Towards a mass table based on covariant density functional theory¹⁾

←

Criteria of drip lines: ↓

$S_n(Sp) < 0$, $S_{2n}(S_{2p}) < 0$, and $\lambda_{n0}(\lambda_{p0}) > 0$ ↓

→

1. To explore the continuum and pairing correlation effects on nucleon drip-lines. ↓

1.1 Spherical symmetry↓

1.2 Fortran program: Relativistic Continuum Hartree Bogoliubov ↓

1.3 Effective interaction: PC-PK1↓

1.4 Pairing force: density-dependent zero-range delta force↓

for given isotopic and/or isotonic chains, and for fixed pairing window↓

increasing the pairing strength gradually, the pairing strength should be determined by

fitting to the experimental even-odd mass differences.↓

1.5 Masses for all nuclei between the proton drip line and the neutron drip line. ↓

a) From O (Z=8) to Ti (Z=22) isotopes: (Completed by Xiaoying Qu, et al.) ↓

b) From Ti (Z=22) to Zn (Z=30) isotopes: (by Dr. Yeunhwan Lim 林年煥, May.09.2013) ↓

c) From Zn (Z=30) to Mo (Z=42) isotopes: (by Dr. Ik Jae Shin 慎翊宰 May.09.2013) ↓

d) From Mo (Z=42) to Te (Z=52) isotopes: ↓

e) From Te (Z=52) to Gd (Z=66) isotopes: ↓

f) From Gd (Z=66) to Po (Z=84) isotopes: ↓

g) From Po (Z=84) to Z=104 isotopes: ↓

h) Superheavy nuclei (Z>104)?↓

1.6 How many nuclei are bound due to the pairing correlation?↓

↑

2. To explore the deformation effects on nucleon drip-lines ↓

↑

↑

3. To explore the beyond mean-field effects on nucleon drip-lines ↓

Lagrangian density of the point-coupling model

$$\mathcal{L} = \mathcal{L}^{free} + \mathcal{L}^{4f} + \mathcal{L}^{hot} + \mathcal{L}^{der} + \mathcal{L}^{em}$$

$$\mathcal{L}^{free} = \bar{\psi}(i\gamma_\mu\partial^\mu - m)\psi,$$

$$\begin{aligned}\mathcal{L}^{4f} = & -\frac{1}{2}\alpha_S(\bar{\psi}\psi)(\bar{\psi}\psi) - \frac{1}{2}\alpha_V(\bar{\psi}\gamma_\mu\psi)(\bar{\psi}\gamma^\mu\psi) \\ & - \frac{1}{2}\alpha_{TS}(\bar{\psi}\vec{\tau}\psi)(\bar{\psi}\vec{\tau}\psi) - \frac{1}{2}\alpha_{TV}(\bar{\psi}\vec{\tau}\gamma_\mu\psi)(\bar{\psi}\vec{\tau}\gamma^\mu\psi),\end{aligned}$$

$$\mathcal{L}^{hot} = -\frac{1}{3}\beta_S(\bar{\psi}\psi)^3 - \frac{1}{4}\gamma_S(\bar{\psi}\psi)^4 - \frac{1}{4}\gamma_V[(\bar{\psi}\gamma_\mu\psi)(\bar{\psi}\gamma^\mu\psi)]^2,$$

$$\begin{aligned}\mathcal{L}^{der} = & -\frac{1}{2}\delta_S\partial_\nu(\bar{\psi}\psi)\partial^\nu(\bar{\psi}\psi) - \frac{1}{2}\delta_V\partial_\nu(\bar{\psi}\gamma_\mu\psi)\partial^\nu(\bar{\psi}\gamma^\mu\psi) \\ & - \frac{1}{2}\delta_{TS}\partial_\nu(\bar{\psi}\vec{\tau}\psi)\partial^\nu(\bar{\psi}\vec{\tau}\psi) \\ & - \frac{1}{2}\delta_{TV}\partial_\nu(\bar{\psi}\vec{\tau}\gamma_\mu\psi)\partial^\nu(\bar{\psi}\vec{\tau}\gamma_\mu\psi),\end{aligned}$$

$$\mathcal{L}^{em} = -\frac{1}{4}F^{\mu\nu}F_{\mu\nu} - e\frac{1-\tau_3}{2}\bar{\psi}\gamma^\mu\psi A_\mu.$$

PC-PK1

Coupling constant	Value	Dimension
α_S	-3.96291×10^{-4}	MeV^{-2}
β_S	8.6653×10^{-11}	MeV^{-5}
γ_S	-3.80724×10^{-17}	MeV^{-8}
δ_S	-1.09108×10^{-10}	MeV^{-4}
α_V	2.6904×10^{-4}	MeV^{-2}
γ_V	-3.64219×10^{-18}	MeV^{-8}
δ_V	-4.32619×10^{-10}	MeV^{-4}
α_{TV}	2.95018×10^{-5}	MeV^{-2}
δ_{TV}	-4.11112×10^{-10}	MeV^{-4}
V_n	-349.5	MeV fm^3
V_p	-330.0	MeV fm^3

Relativistic Dirac-Hartree-Bogoliubov equation Kucharek and Ring, Z. Phys. A 339, 23 (1991)

$$\begin{pmatrix} h_D - \lambda & \Delta \\ -\Delta^* & -h_D^* + \lambda \end{pmatrix} \begin{pmatrix} U_k \\ V_k \end{pmatrix} = E_k \begin{pmatrix} U_k \\ V_k \end{pmatrix}$$

Dirac Hamiltonian

$$h_D = \boldsymbol{\alpha} \cdot \boldsymbol{p} + \beta(M + S(r)) + V(r)$$

where scalar and vector potentials

$$S(r) = \alpha_S \rho_S + \beta_S \rho_S^2 + \gamma_S \rho_S^3 + \delta_S \Delta_{\rho_S}$$

$$V(r) = \alpha_V \rho_V + \gamma_V \rho_V^3 + \delta_V \Delta_{\rho_V} + eA_0 + \alpha_{TV} \tau_3 \rho_{TV} + \delta_{TV} \tau_3 \Delta_{TV}$$

with local densities

$$\rho_S = \sum_{k>0} \bar{V}_k(r) V_k(r)$$

$$\rho_V = \sum_{k>0} V_k^+(r) V_k(r)$$

$$\rho_{TV} = \sum_{k>0} V_k^+(r) \tau_3 V_k(r)$$

The pairing potential Δ

$$\Delta(\mathbf{r}_1, \mathbf{r}_2) = V^{\text{PP}}(\mathbf{r}_1, \mathbf{r}_2)\kappa(\mathbf{r}_1, \mathbf{r}_2),$$

a density-dependent force of zero range,

$$V^{\text{PP}}(\mathbf{r}_1, \mathbf{r}_2) = V_0 \frac{1}{2} (1 - P^\sigma) \delta(\mathbf{r}_1 - \mathbf{r}_2) \left(1 - \frac{\rho(\mathbf{r}_1)}{\rho_{\text{sat}}}\right)$$

For axially deformed nuclei, the potentials and densities are expanded in terms of the Legendre polynomials,

$$f(\mathbf{r}) = \sum_{\lambda} f_{\lambda}(r) P_{\lambda}(\cos \theta), \quad \lambda = 0, 2, 4, \dots,$$

where λ is restricted to be even numbers due to spatial reflection symmetry.

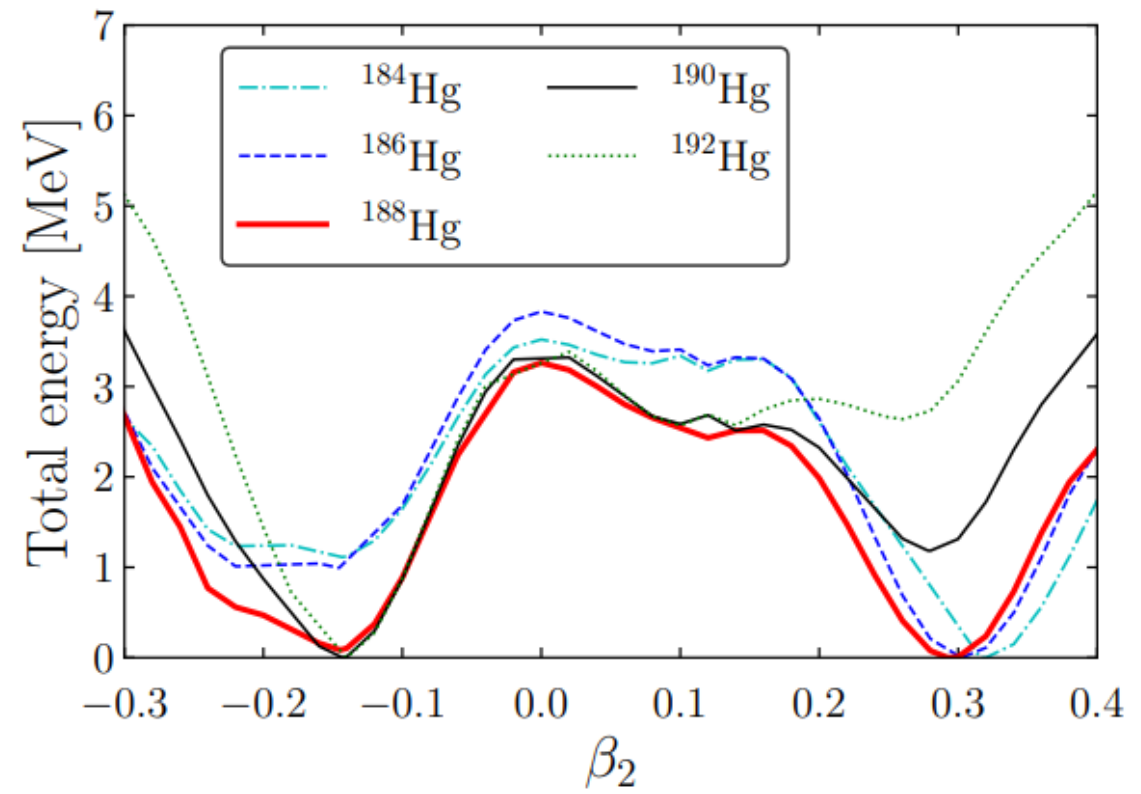
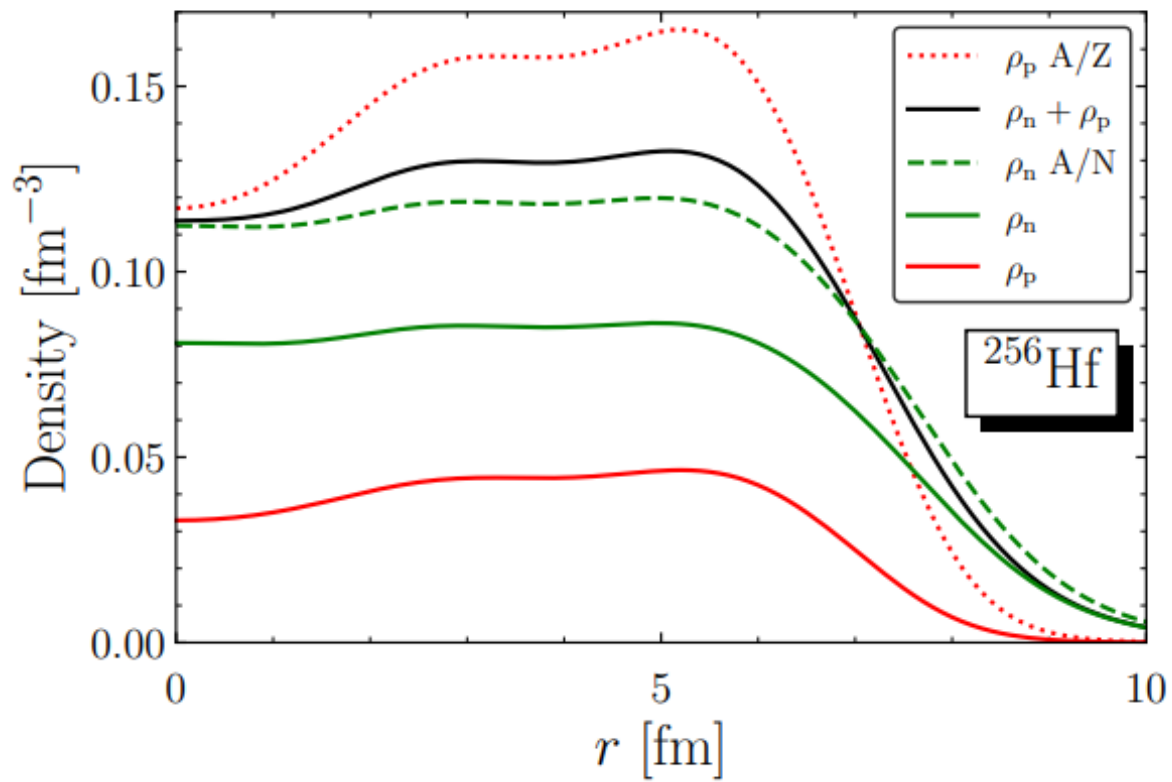
TABLE III. List of the isotopes with both bubble structure and shape coexistence. $|\Delta E|$ is the absolute value of the energy difference between prolate and oblate shapes.

Nucleus	Prolate shape		Oblate shape		$ \Delta E $ [MeV]
	β_2	\mathcal{B}_p^* [%]	β_2	\mathcal{B}_p^* [%]	
^{202}Hf	+0.100	23.7	-0.072	22.4	0.214
^{234}Hf	+0.272	20.5	-0.234	2.4	0.263
^{236}Hf	+0.262	20.4	-0.227	2.2	0.318
^{240}Hf	+0.241	21.0	-0.192	3.5	0.468
^{250}Hf	+0.091	24.0	-0.086	18.3	0.171
^{194}W	+0.136	23.1	-0.126	12.1	0.155
^{204}W	+0.080	23.8	-0.060	22.8	0.087
^{254}W	+0.068	24.2	-0.060	21.7	0.401
^{196}Os	+0.123	23.6	-0.119	11.0	0.096
^{206}Os	+0.044	24.1	-0.042	23.5	0.006
^{208}Os	+0.112	22.4	-0.079	20.4	0.447
^{256}Os	+0.058	24.0	-0.065	20.6	0.141
^{210}Pt	+0.072	22.5	-0.061	21.4	0.016
^{212}Pt	+0.113	21.0	-0.080	19.6	0.404

$$\mathcal{B}_p \equiv \left(1 - \frac{\rho_{p,c}}{\rho_{p,\max}}\right) \times 100 [\%].$$

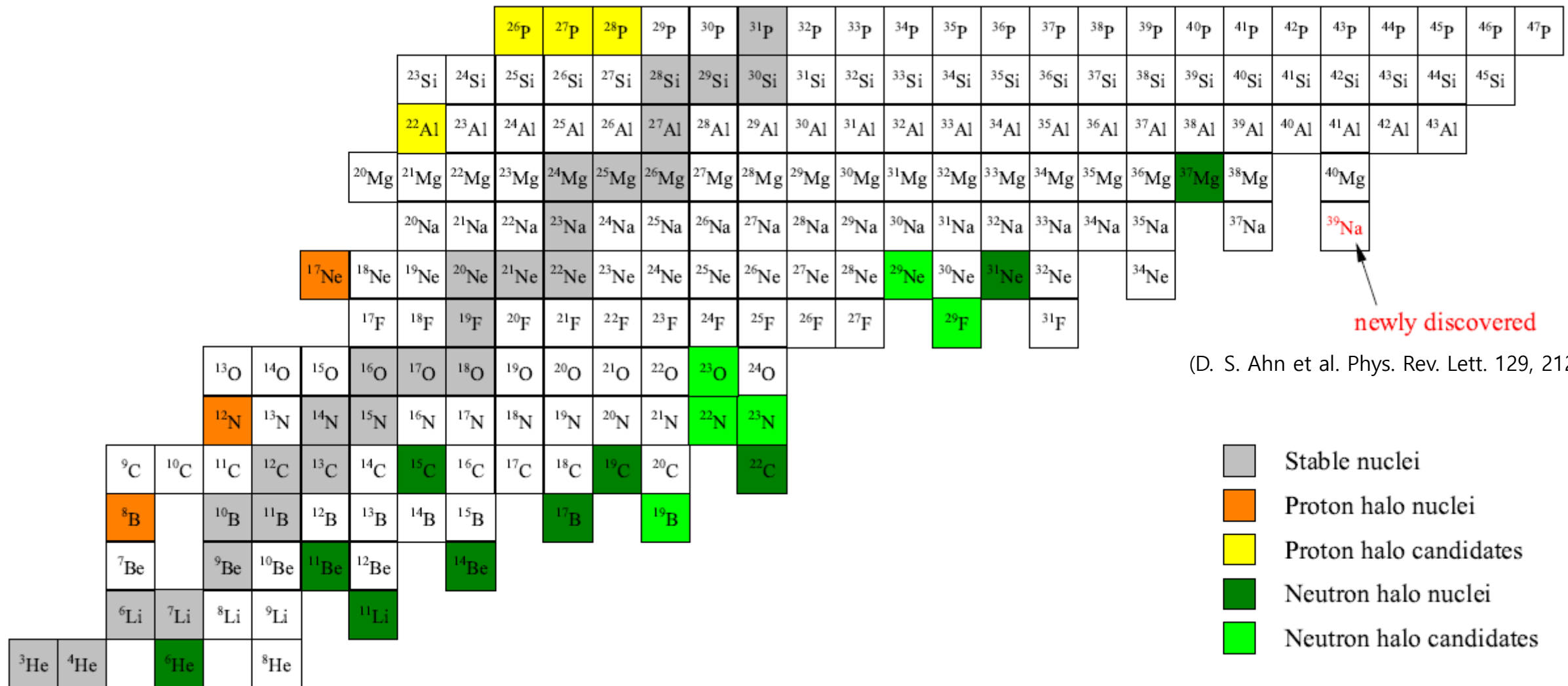
$$\mathcal{B}_p^* \equiv \left(1 - \frac{\bar{\rho}_{p,c}}{\bar{\rho}_{p,\max}}\right) \times 100\%.$$

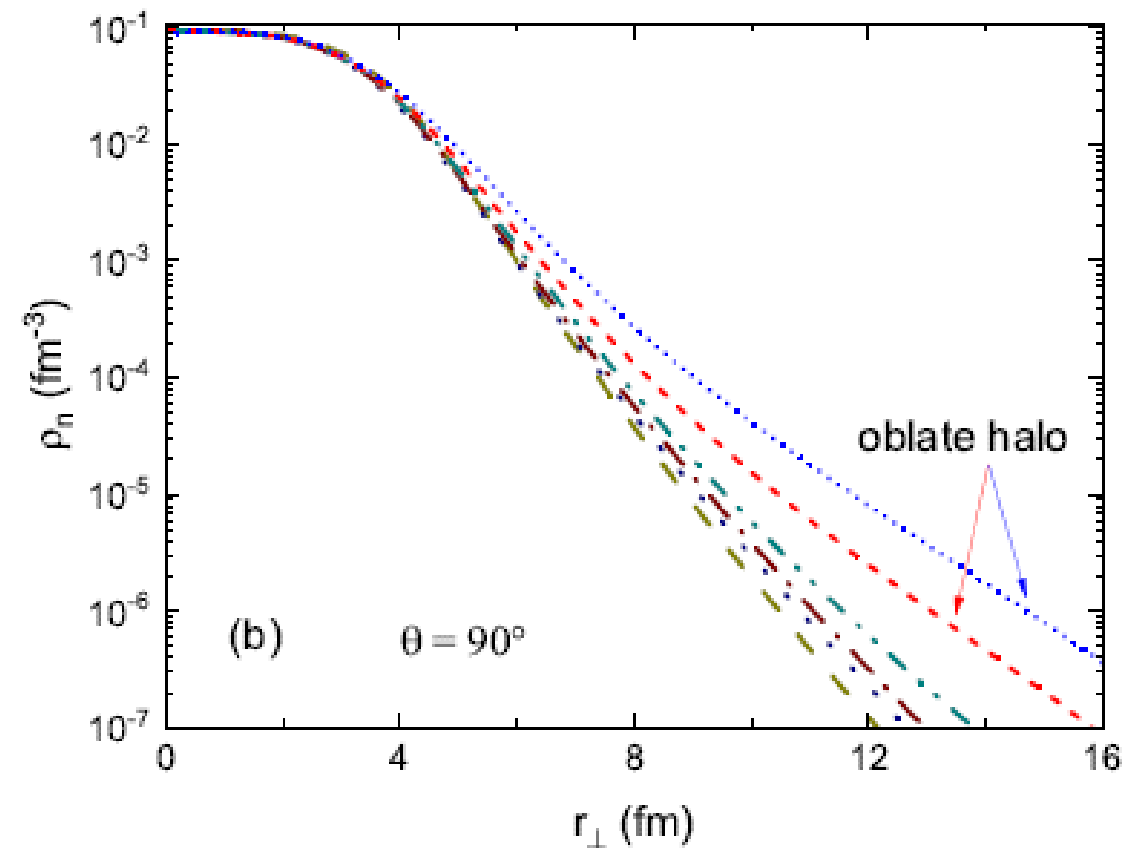
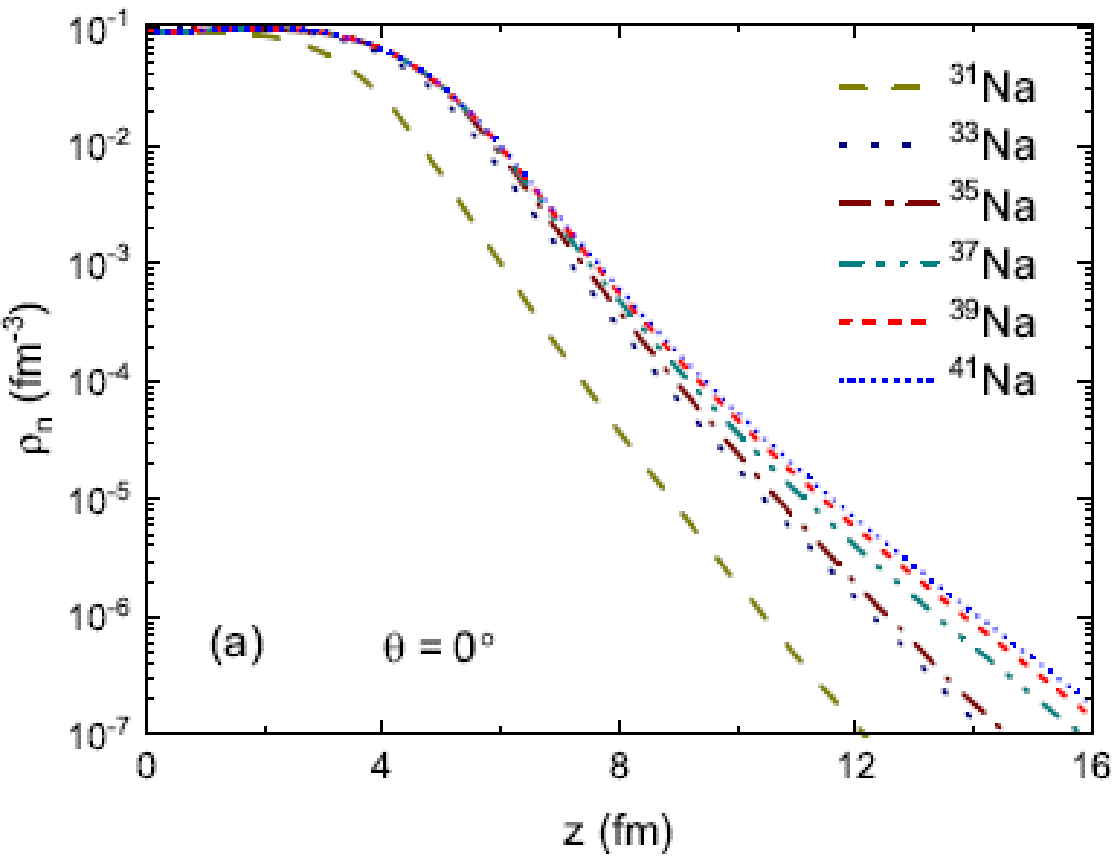
$$\bar{\rho}_{p,\max} = \frac{\int \rho_p(r, \theta) \delta(r - r_{\max}(\theta)) dV}{\int \delta(r - r_{\max}(\theta)) dV}$$



Collapse of the $N = 28$ shell closure in the newly discovered ^{39}Na and the development of deformed halos towards the neutron dripline

Halos and changes of nuclear magicities have been extensively investigated in exotic nuclei during past decades. The newly discovered ^{39}Na with the neutron number $N = 28$ provides a new platform to explore such novel phenomena near the neutron dripline of sodium isotopic chain. We study the shell property and the possible halo structure in ^{39}Na within the deformed relativistic Hartree-Bogoliubov theory in continuum. It is found that the near degeneracy of the $1f_{7/2}$ and $2p_{3/2}$ orbitals in the spherical limit results in the collapse of the $N = 28$ shell closure in ^{39}Na , and a well deformed ground state is established. The pairing correlations and the mixing of pf components driven by deformation lead to the occupation of weakly bound or continuum p -wave neutrons. An oblate halo is therefore formed around the prolate core in $^{39,41}\text{Na}$, making ^{39}Na a single nucleus with the coexistence of several exotic structures, including the quenched $N = 28$ shell closure, the deformed halo, and the shape decoupling. The microscopic mechanisms behind the shape decoupling phenomenon and the development of halos towards dripline are revealed.







Contents lists available at [ScienceDirect](#)

Atomic Data and Nuclear Data Tables

journal homepage: www.elsevier.com/locate/adt

The limits of the nuclear landscape explored by the relativistic continuum Hartree–Bogoliubov theory

X.W. Xia^a, Y. Lim^{b,c}, P.W. Zhao^{d,e}, H.Z. Liang^f, X.Y. Qu^{a,g}, Y. Chen^{d,h}, H. Liu^d, L.F. Zhang^d, S.Q. Zhang^d, Y. Kim^c, J. Meng^{d,a,i,*}

Atomic Data and Nuclear Data Tables 144 (2022) 101488



Contents lists available at [ScienceDirect](#)

Atomic Data and Nuclear Data Tables

journal homepage: www.elsevier.com/locate/adt

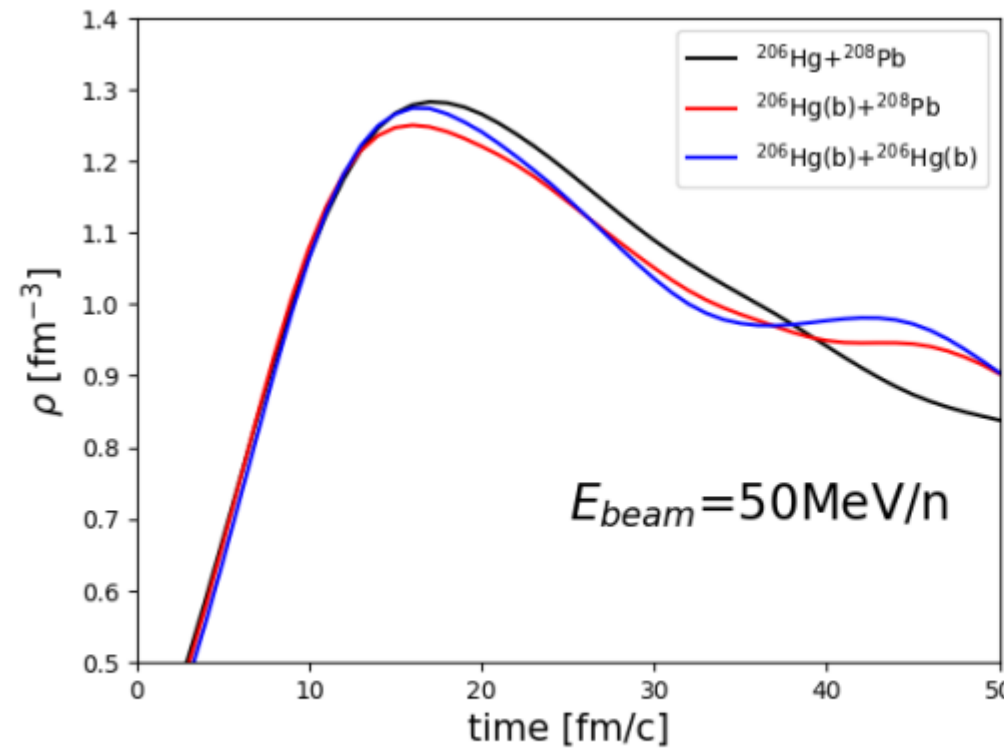
Nuclear mass table in deformed relativistic Hartree–Bogoliubov theory in continuum, I: Even–even nuclei

Kaiyuan Zhang^a, Myung-Ki Cheoun^b, Yong-Beom Choi^c, Pooi Seong Chong^d, Jianmin Dong^{e,f}, Zihao Dong^a, Xiaokai Du^a, Lisheng Geng^{g,h}, Eunja Haⁱ, Xiao-Tao He^j, Chan Heo^d, Meng Chit Ho^d, Eun Jin In^{k,l}, Seonghyun Kim^b, Youngman Kim^m, Chang-Hwan Lee^c, Jenny Lee^d, Hexuan Li^a, Zhipan Liⁿ, Tianpeng Luo^a, Jie Meng^{a,*}, Myeong-Hwan Mun^{b,o}, Zhongming Niu^p, Cong Pan^a, Panagiota Papakonstantinou^m, Xinle Shang^{e,f}, Caiwan Shen^q, Guofang Shen^g, Wei Sunⁿ, Xiang-Xiang Sun^{r,s}, Chi Kin Tam^d, Thaivayongnou^g, Chen Wang^j, Xingzhi Wang^a, Sau Hei Wong^d, Jiawei Wu^j, Xinhui Wu^a, Xuewei Xia^t, Yijun Yan^{e,f}, Ryan Wai-Yen Yeung^d, To Chung Yiu^d, Shuangquan Zhang^a, Wei Zhang^h, Xiaoyan Zhang^p, Qiang Zhao^{k,a}, Shan-Gui Zhou^{s,u,v,w}, DRHBc Mass Table Collaboration

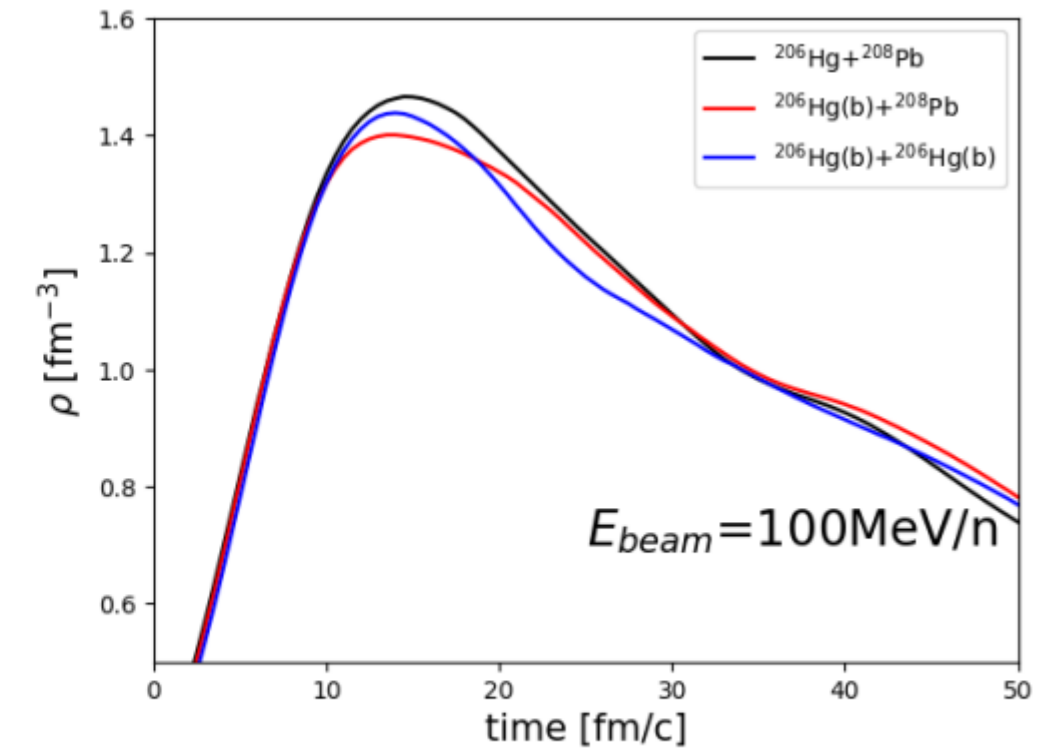
Nuclear mass table in deformed relativistic Hartree-Bogoliubov theory in continuum, II: Even- Z nuclei

Peng Guo,¹ Xiaojie Cao,² Zhihui Chen,³ Myung-Ki Cheoun,⁴ Yong-Beom Choi,⁵ Lam Pak Chung,³ Jianmin Dong,^{6,7} Xiaokai Du,¹ Kangda Duan,⁶ Xiaohua Fan,⁸ Wei Gao,⁹ Lisheng Geng,^{10,9} Eunja Ha,¹¹ Xiao-Tao He,¹² Jinniu Hu,¹³ Jingke Huang,⁹ Kun Huang,¹² Zidan Huang,⁹ Kim Da Hyung,³ Chan Hoi Yat Jeffrey,³ Xiaofei Jiang,¹ Seonghyun Kim,⁴ Youngman Kim,¹⁴ Chang-Hwan Lee,⁵ Jenny Lee,³ Minglong Li,¹⁵ Zhipan Li,¹⁶ Haozhao Liang,^{15,17} Lang Liu,¹⁸ Xiao Lu,¹⁹ Zhi-Rui Liu,¹² Jie Meng,^{1,*} Ziyan Meng,¹ Myeong-Hwan Mun,^{4,20} Yifei Niu,²¹ Zhongming Niu,²² Cong Pan,^{1,23} Xiaoying Qu,²⁴ Panagiota Papakonstantinou,²⁵ Xinle Shang,^{6,7} Caiwan Shen,²⁶ Guofang Shen,¹⁰ Tingting Sun,⁹ Wei Sun,¹⁶ Xiang-Xiang Sun,^{27,19} Tianyu Wang,²⁸ Yiran Wang,² Jiawei Wu,¹² Liang Wu,⁹ Xinhui Wu,²⁹ Xuewei Xia,³⁰ Jiangming Yao,^{31,32} Tammi Ip Kwan Yau,³ To Chung Yiu,³ Jianghan Yu,²⁶ Kaiyuan Zhang,^{1,33} Shijie Zhang,⁹ Shuangquan Zhang,¹ Wei Zhang,⁹ Xiaoyan Zhang,²² Yanxin Zhang,³¹ Ying Zhang,² Qiang Zhao,^{14,1} Yingchun Zhao,¹ Ruyou Zheng,¹⁰ Chang Zhou,¹ Shan-Gui Zhou,^{19,34,27,35} and Lianjian Zou¹³

DaeJeon–Boltzmann–Uehling–Uhlenbeck (DJBUU)

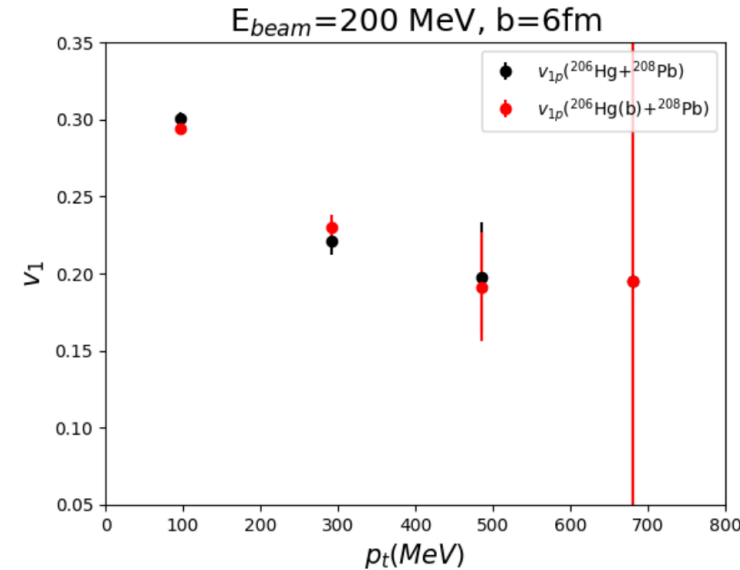
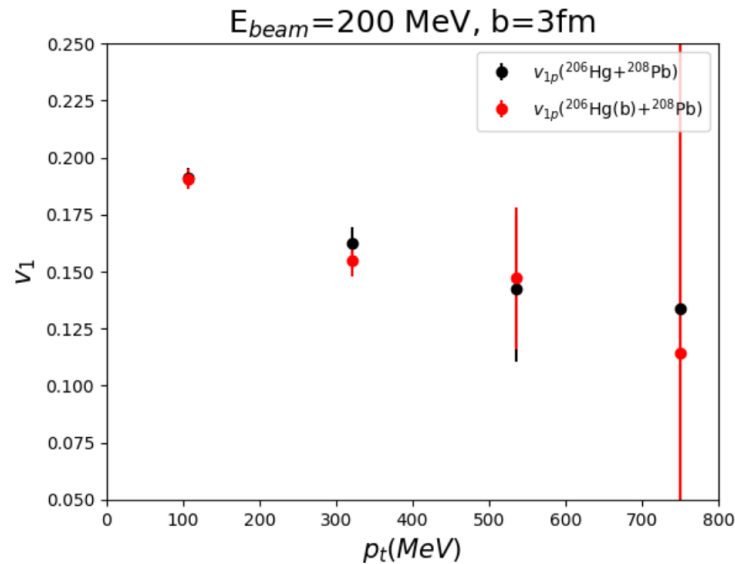
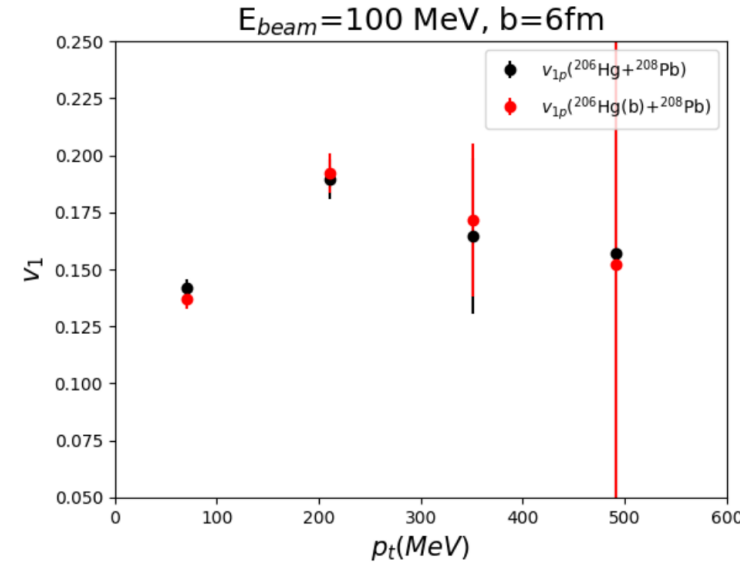
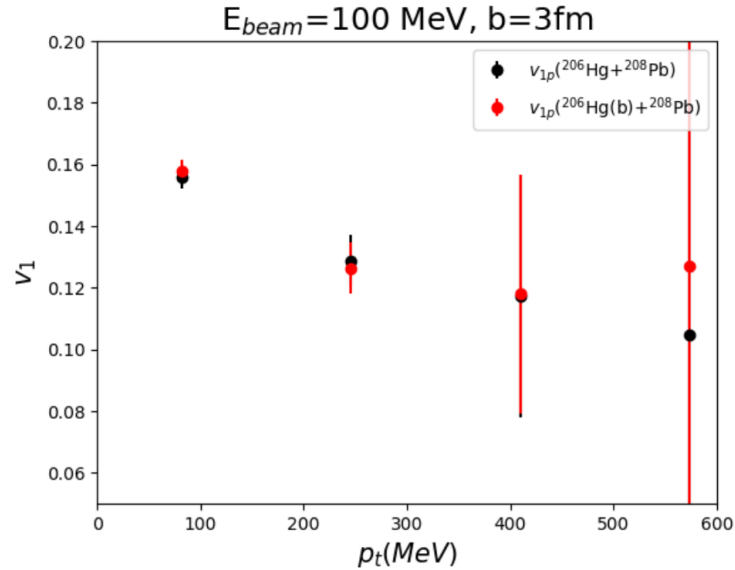


(a)



(b)

The densities at the collision center at $E_{beam} = 50$ (a) and 100 (b) MeV when the impact parameter is 3 fm



The directed flow v_1 of protons

Table 1. π^- / π^+ ratio at $E_{beam} = 300$ A MeV.

b	$^{206}\text{Hg} + ^{208}\text{Pb}$	$^{206}\text{Hg (Bubble)} + ^{208}\text{Pb}$	$^{206}\text{Hg (Bubble)} + ^{206}\text{Hg (Bubble)}$
0 fm	3.18 (± 0.11)	3.10 (± 0.08)	3.30 (± 0.10)
3 fm	3.18 (± 0.11)	3.22 (± 0.06)	3.23 (± 0.07)
6 fm	3.32 (± 0.10)	3.08 (± 0.16)	3.37 (± 0.17)

Parity doublet model in finite nuclei

- ✓ Spherical code was provided by Prof. Jie Meng (Peking Univ.).
- ✓ Main difference is the behavior of sigma mean field.
- ✓ Revised the code to incorporate the difference.
- ✓ With no Delta baryons in matter
- ✓ Can we pin down the value of the chiral invariant mass?

The equations of motion (EoM) for the stationary mean fields $\tilde{\sigma}$, ω_0 , ρ_0^3 and A_0 read

$$\begin{aligned} \left(-\vec{\nabla}^2 + m_\sigma^2 \right) \langle \tilde{\sigma}(\vec{x}) \rangle &= -\bar{N}(\vec{x}) N(\vec{x}) \left. \frac{\partial m_N(\tilde{\sigma})}{\partial \tilde{\sigma}} \right|_{\tilde{\sigma}=\langle \tilde{\sigma}(\vec{x}) \rangle} \\ &\quad + (-3f_\pi\lambda + 10f_\pi^3\lambda_6) \langle \tilde{\sigma}(\vec{x}) \rangle^2 \\ &\quad + (-\lambda + 10f_\pi^2\lambda_6) \langle \tilde{\sigma}(\vec{x}) \rangle^3 \\ &\quad + 5f_\pi\lambda_6 \langle \tilde{\sigma}(\vec{x}) \rangle^4 + \lambda_6 \langle \tilde{\sigma}(\vec{x}) \rangle^5, \\ \left(-\vec{\nabla}^2 + m_\omega^2 \right) \langle \omega_0(\vec{x}) \rangle &= g_{\omega NN} N^\dagger(\vec{x}) N(\vec{x}), \\ \left(-\vec{\nabla}^2 + m_\rho^2 \right) \langle \rho_0^3(\vec{x}) \rangle &= g_{\rho NN} N^\dagger(\vec{x}) \tau^3 N(\vec{x}), \\ -\vec{\nabla}^2 \langle A_0(\vec{x}) \rangle &= e N^\dagger(\vec{x}) \frac{1 - \tau_3}{2} N(\vec{x}). \end{aligned}$$

The EoM for the nucleon is given by

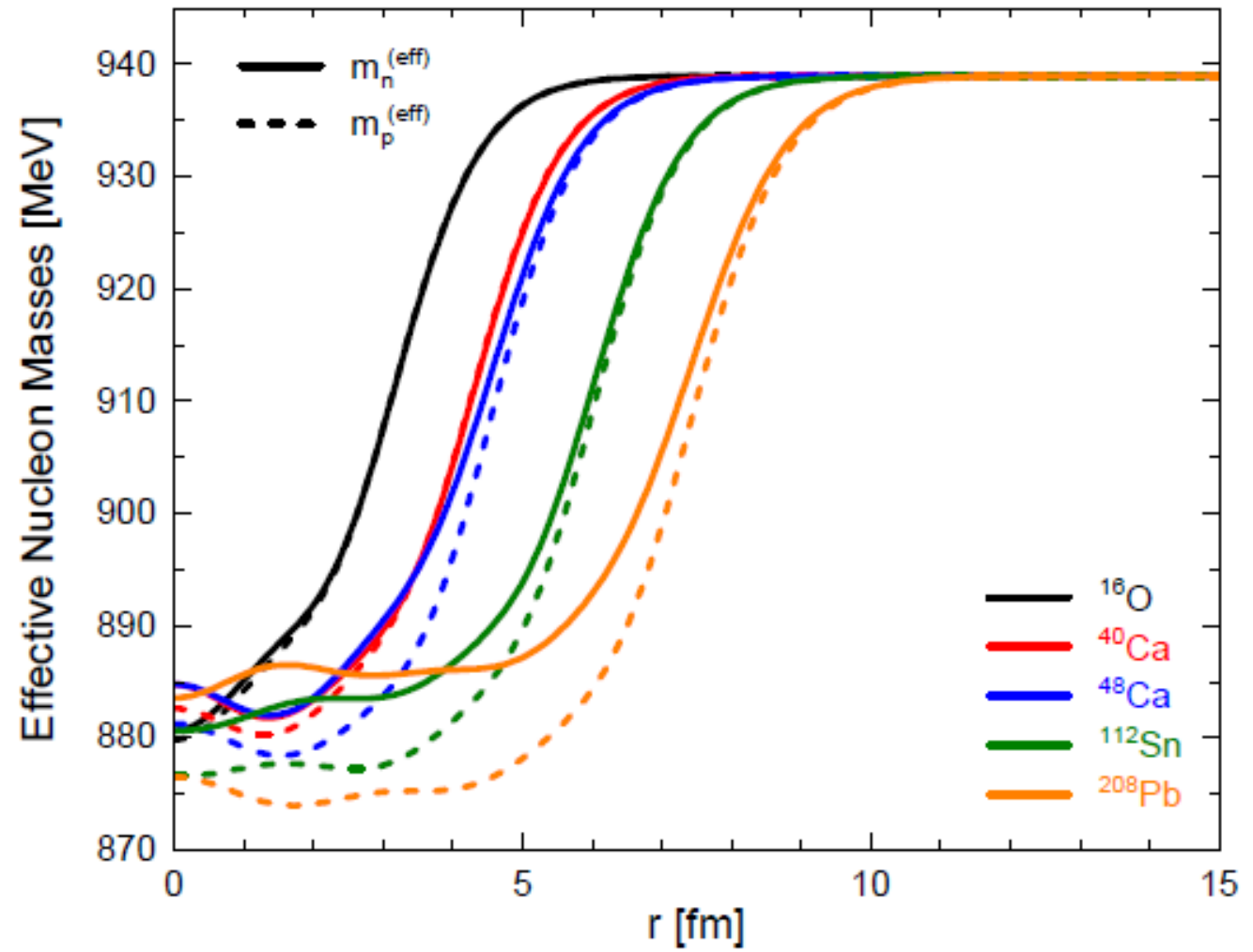
$$[\vec{\alpha} \cdot \vec{p} + \beta m_N(\langle \tilde{\sigma}(\vec{x}) \rangle) + V(\vec{x})] N_i(\vec{x}) = \epsilon_i N_i(\vec{x}),$$

$$V(\vec{x}) = g_{\omega NN} \langle \omega_0(\vec{x}) \rangle + g_{\rho NN} \langle \rho_0^3(\vec{x}) \rangle \tau^3 + e \frac{(1 - \tau_3)}{2} \langle A_0(\vec{x}) \rangle.$$

m_0 (MeV)		600	700	800	900	Exp.
BE/A (MeV)	^{16}O	7.087	7.280	6.792	5.093	7.976
	^{40}Ca	7.736	7.906	7.538	6.191	8.551
	^{48}Ca	7.676	7.768	7.378	6.061	8.667
	^{58}Ni	7.391	7.486	7.108	5.849	8.732
	^{70}Ge	7.761	7.900	7.584	6.429	8.722
	^{82}Se	7.799	7.899	7.580	6.462	8.693
	^{92}Mo	7.741	7.821	7.507	6.424	8.658
	^{112}Sn	7.668	7.760	7.474	6.460	8.514
	^{126}Sn	7.757	7.801	7.516	6.536	8.443
	^{138}Ba	7.695	7.758	7.482	6.526	8.393
	^{154}Sm	7.596	7.691	7.447	6.540	8.227
	^{170}Er	7.526	7.587	7.354	6.484	8.112
	^{182}W	7.418	7.466	7.237	6.387	8.018
RMS deviation	^{202}Pb	7.277	7.303	7.062	6.221	7.882
	^{208}Pb	7.306	7.322	7.075	6.232	7.867
RMS deviation		0.827	0.737	1.047	2.147	—

m_0 (MeV)		600	700	800	900	Exp.
R_C (fm)	^{16}O	2.877	2.792	2.790	2.803	2.699
	^{40}Ca	3.572	3.491	3.485	3.479	3.478
	^{48}Ca	3.605	3.537	3.532	3.522	3.478
	^{58}Ni	3.932	3.863	3.861	3.855	3.776
	^{70}Ge	4.104	4.028	4.018	4.001	4.041
	^{82}Se	4.223	4.154	4.145	4.125	4.140
	^{92}Mo	4.418	4.351	4.347	4.335	4.315
	^{112}Sn	4.684	4.616	4.608	4.591	4.594
	^{126}Sn	4.764	4.703	4.695	4.675	4.685
	^{138}Ba	4.928	4.865	4.856	4.834	4.838
	^{154}Sm	5.117	5.045	5.031	5.004	5.105
	^{170}Er	5.250	5.181	5.169	5.144	5.279
	^{182}W	5.374	5.305	5.294	5.270	5.356
	^{202}Pb	5.555	5.493	5.485	5.462	5.471
	^{208}Pb	5.588	5.529	5.521	5.499	5.501
RMS deviation		0.097	0.052	0.053	0.062	—

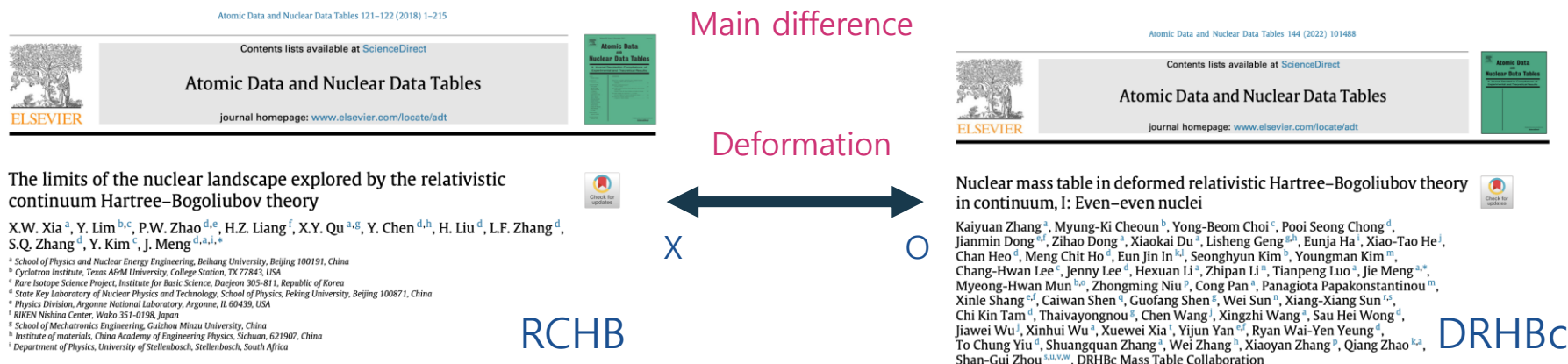
	BE/A (MeV)			R_C (fm)		
	PDM	RCHB	Exp.	PDM	RCHB	Exp.
^{16}O	8.040	7.956	7.976	2.757	2.768	2.699
^{40}Ca	8.574	8.577	8.551	3.464	3.481	3.478
^{48}Ca	8.419	8.654	8.667	3.517	3.494	3.478
^{58}Ni	8.118	8.691	8.732	3.843	3.737	3.776
^{70}Ge	8.521	8.650	8.722	4.010	4.001	4.041
^{82}Se	8.513	8.664	8.693	4.142	4.125	4.140
^{92}Mo	8.408	8.662	8.658	4.335	4.310	4.315
^{112}Sn	8.339	8.489	8.514	4.605	4.582	4.594
^{126}Sn	8.372	8.447	8.443	4.695	4.683	4.685
^{138}Ba	8.329	8.406	8.393	4.860	4.848	4.838
^{154}Sm	8.263	8.149	8.227	5.042	5.062	5.105
^{170}Er	8.140	8.000	8.112	5.176	5.224	5.279
^{182}W	8.007	7.927	8.018	5.299	5.342	5.356
^{202}Pb	7.837	7.869	7.882	5.491	5.490	5.471
^{208}Pb	7.860	7.875	7.867	5.529	5.518	5.501
RMS deviation	0.204	0.05	—	0.045	0.031	—



Possible effects of nuclear deformations on the solar r-abundances

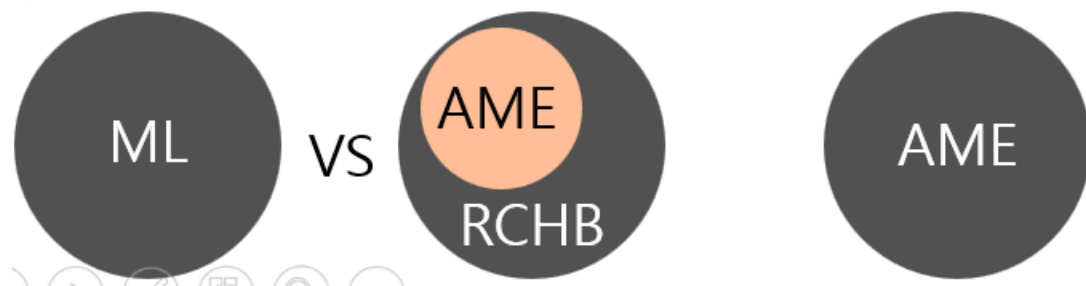
1. Construction the neural network.
 2. Training using AME2020+RCHB (even-even, even-odd) data and compare the AME2020+RCHB whole data.
We expect that the machine might learn the odd information from AME2020 data.
 3. Training using AME2020+DRHBc (even-even, even-odd) data and predict the odd-even, odd-odd cases.

We expect that the machine might learn the odd information from AME2020 data.



Input data: N, Z

Layer-node	RMS deviation (AME+RCHB)	RMS deviation (AME)
32-32	5.1592	2.7485
48-48-48	2.2155	1.7794
64-64	2.7032	2.9272

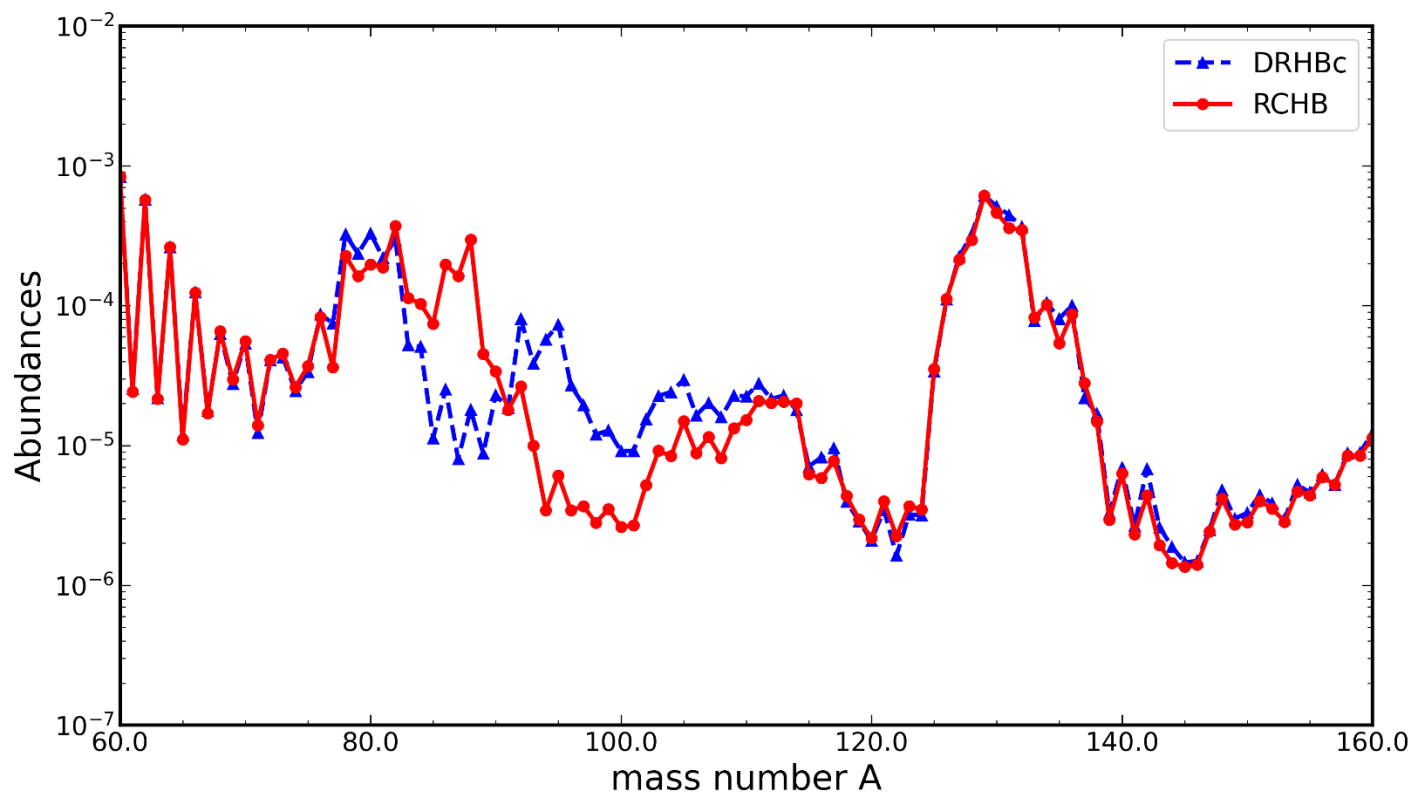


5-inputs DRHBC*

Layer-node	RMS deviation (AME+DRHBC)	RMS deviation (AME)
48-48-48	1.6629	0.8417
64-64	1.6500	1.2817

5-inputs RCHB*

Layer-node	RMS deviation (AME+RCHB)	RMS deviation (AME)
48-48-48	1.9567	1.8617
64-64	2.2422	1.7049



Soon-Chul Choi, Kyungil Kim, YK and T. Kajino, in progress

Summary

- Focusing on nuclear structures, recent results from ab initio or microscopic theories were discussed
- For compound nuclear reactions we have used DNS model. Recently, we started to work with the Langevin method.
- For direct nuclear reactions, ... so far some but not much ...